

ABSTRACT

Title of Thesis: SYNTHESIS AND CHARACTERIZATION OF
OLIGOSACCHARIDES TETHERED TO
GOLD FILMS AND NANOPARTICLES

Mridula Kadalbajoo, Master of Science, 2004

Thesis Directed By: Professor Philip DeShong
Department of Chemistry and Biochemistry

The goal of this research was to stereoselectively synthesize α - and β - linked glucopyranosylamide derivatives utilizing the modified Staudinger methodology and to tether these derivatives to gold films and gold nanoparticles. The key step in the synthesis of the glucopyranosyl conjugates is the coupling of a glycosylazide to an acid derivative in the presence of either triphenylphosphine or trimethylphosphine. The synthesis proceeds via the in situ generation of glucosyl isoxazoline intermediate. The characterization of the resulting films and particles has been performed using Fourier-Transform Infrared (FT-IR), Atomic Force Microscopy (AFM), and X-Ray Photoelectron Spectroscopy (XPS). The XPS and AFM analyses have shown evidence for monolayer and multilayered films depending on the derivative used. Glucopyranosyl derivatives with free hydroxyl groups gave well ordered, self-assembled monolayers (SAMs). FT-IR and XPS analysis of the SAMs demonstrated that the resulting monolayers were comprised of a hydrogen bonded network between amides on adjacent sites.

Glycoconjugates have also been attached to gold nanoparticles and evidence for aggregation of gold nanoparticles when bound to hydroxylated glycosylamides having thiolated/disulfide side chains has been observed. There is evidence for an enhancement in the aggregation of the gold nanoparticles in the presence of the lectin Concanavalin A which binds specifically to α -linked gluco and mannopyranosides.

SYNTHESIS AND CHARACTERIZATION OF OLIGOSACCHARIDES
TETHERED TO GOLD FILMS AND GOLD NANOPARTICLES

By

Mridula Kadalbajoo

Thesis submitted to the Faculty of the Graduate School of the
University of Maryland, College Park, in partial fulfillment
of the requirements for the degree of
Master of Science
2004

Advisory Committee:
Professor Philip DeShong, Chair
Professor Daniel Falvey
Professor Steven Rokita
Professor Neil Blough

© Copyright by
Mridula Kadalbajoo
2004

ACKNOWLEDGEMENT

My sincerest thanks to my advisor Dr. Philip DeShong for his support and guidance throughout. I would also like to thank the DeShong group members, new and old, for their help and companionship. Special thanks to my mentors Dr. Reuben Correia and Dr. Fehmi Damkaci for always being there for me and guiding me. Last but not the least I would like to thank my parents for their faith in me and their unconditional love and support.

TABLE OF CONTENTS

| | |
|---|------|
| List of Tables | iv |
| List of Figures | v |
| List of Schemes | vi |
| List of Abbreviations | vii |
| List of Abbreviations | viii |
| Introduction | 1 |
| Goals of My Research | 16 |
| Results and Discussion | 17 |
| 1) Synthesis of N-linked Glycosylamides | 17 |
| 2) Gold Films | 24 |
| 3) Gold Nanoparticles | 34 |
| Conclusion | 38 |
| Experimental | 39 |
| Appendix | 59 |
| References | 60 |

LIST OF TABLES

| | | |
|----------|---|----|
| Table 1. | Coupling Reactions using modified Staudinger Methodology. | 9 |
| Table 2. | Hydroxylation Reaction for Oligosaccharides. | 24 |
| Table 3. | Results of XPS analysis of Monolayers on Gold. | 30 |
| Table 4. | Contact Angles for oligosaccharides. | 34 |

LIST OF FIGURES

| | | |
|------------|--|----|
| Figure 1. | Convergent Approach to the synthesis of oligosaccharides. | 2 |
| Figure 2. | Stepwise Approach to the synthesis of oligosaccharides. | 2 |
| Figure 3. | FT-IR of α -Glu-OAc-CH ₃ at 2 h and 20 h. | 26 |
| Figure 4. | FT-IR of α -Glu-OAc-SH at 2 h and 20 h. | 26 |
| Figure 5. | FT-IR of α -Glu-OH-SH at 2 h and 20 h. | 26 |
| Figure 6. | FT-IR of α -Glu-OH-S ₂ at 2 h and 20 h. | 27 |
| Figure 7. | FT-IR of β -Glu-OH-S ₂ at 2 h and 20 h. | 28 |
| Figure 8. | Comparison of oligosaccharide SAMs after 2 and 20 h immersion. | 29 |
| Figure 9. | Proposed mechanism for ordered monolayer formation. | 31 |
| Figure 10. | S/Au ratios for acetylated and hydroxylated oligosaccharides. | 32 |
| Figure 11. | N/Au ratios for acetylated and hydroxylated oligosaccharides. | 32 |
| Figure 12. | Comparison of nitrogen (non-H bonded) and nitrogen (H-bonded). | 33 |
| Figure 13. | TEM of Au nanoparticles prior to surface functionalization. | 35 |
| Figure 14. | TEM of aggregates of Au nanoparticles functionalized with α -glucopyranosylamide. | 35 |
| Figure 15. | TEM of Au nanoparticles prior to surface functionalization. | 36 |
| Figure 16. | TEM of dilution experiment of Au nanoparticles. | 37 |

LIST OF SCHEMES

| | |
|-----------|----|
| Scheme 1 | 3 |
| Scheme 2 | 4 |
| Scheme 3 | 5 |
| Scheme 4 | 5 |
| Scheme 5 | 6 |
| Scheme 6 | 6 |
| Scheme 7 | 7 |
| Scheme 8 | 7 |
| Scheme 9 | 8 |
| Scheme 10 | 10 |
| Scheme 11 | 11 |
| Scheme 12 | 18 |
| Scheme 13 | 18 |
| Scheme 14 | 19 |
| Scheme 15 | 19 |
| Scheme 16 | 20 |
| Scheme 17 | 21 |
| Scheme 18 | 21 |
| Scheme 19 | 22 |
| Scheme 20 | 23 |

LIST OF ABBREVIATIONS

| | |
|--------|---|
| Ar | Aryl |
| Ac | Acetyl |
| AFM | Atomic force microscopy |
| Equiv. | Equivalent |
| FT-IR | Fourier transform infrared spectroscopy |
| H | Hour (s) |
| Hz | Hertz |
| IR | Infrared |
| NMR | Nuclear Magnetic Resonance |
| TLC | Thin Layer Chromatography |
| UV | Ultraviolet |
| Con A | Concanavalin A |

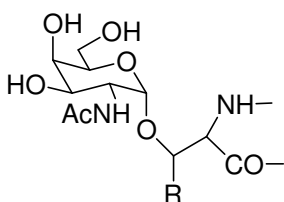
LIST OF ABBREVIATIONS

| Oligosaccharides | Names |
|------------------|----------------------------------|
| | α -glu-OAc-SH |
| | α -glu-OH-SH |
| | α -glu-OAc-S ₂ |
| | α -glu-OH-S ₂ |
| | α -mal-OAc-S ₂ |
| | α -mal-OH-S ₂ |

Introduction

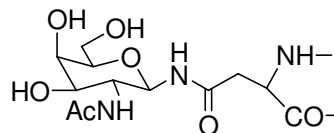
Oligosaccharides and glycoconjugates (glycolipids and glycoproteins) have intrigued chemists and biologists for a long time because of their crucial role in inflammation, immune response, metastasis, fertilization and many other biomedically important processes.¹ In particular, the interest in glycoproteins has grown over the years due to their biologically important roles such as cell recognition, cell adhesion and cell growth regulation.²

Glycoproteins are divided into two groups that are differentiated by the type of linkage between the carbohydrate and the protein: N-glycosidic glycoproteins and O-glycosidic glycoproteins.



O-linked glycoproteins

R = H (serine)
= CH₃ (threonine)



N-linked glycoproteins

In this paper we will focus on the N-linked glycopeptides, which can be made via a number of different strategies.

Synthetic Strategies for Glycoproteins

The most important step of any synthesis of a glycopeptide is the introduction of a

carbohydrate residue to the amino acid in a stereoselective manner. This should be done under conditions that do not affect the existing glycosidic linkages and also are compatible with commonly used protecting groups.

a) Convergent approach: An oligosaccharide moiety and a peptide moiety are prepared separately, then coupled with each other. Commonly this approach is used for the preparation of N-glycopeptides.^{3,4}



Figure 1. Convergent approach

b) StepWise approach: Glycosylamino acids are used as a building block for solid phase synthesis. This approach is effective for the synthesis glycopeptides either with a single carbohydrate or multiple carbohydrates.

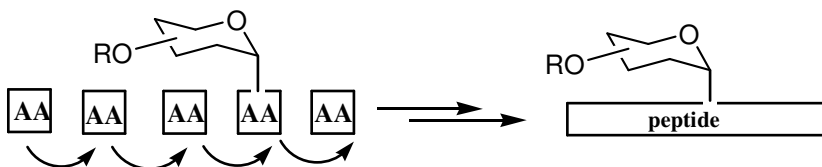


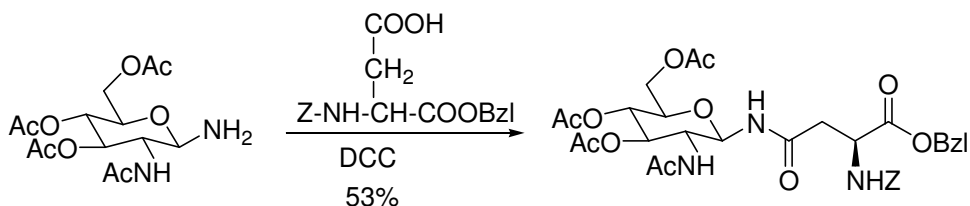
Figure 2. Stepwise approach

I. Via Glycosyl Amines

One of the methods to make the β -N glycosidic linkage between N-acetylglucosamine and asparagine which is characteristic of N-glycoproteins is by the condensation of N-protected aspartic acid monoesters and 2-acetamido-3, 4, 6-tri-O-acetyl-2-deoxy- β -

D-glucopyranosylamine in the presence of a coupling reagent like dicyclohexylcarbodiimide (DCC) (Scheme 1).⁵

Scheme 1



Glycosylamines can be synthesized from the reaction of an unprotected carbohydrate with aqueous ammonium hydrogen carbonate^{6,7} or the catalytic reduction of the corresponding azide using Pd/C^{8,9}, Lindlar catalyst¹⁰, PtO₂¹¹, Raney Ni¹², Al/Hg, or 1, 3 propanedithiol.^{13,14} Both these methods however, pose problems due to the formation of undesired by-products.

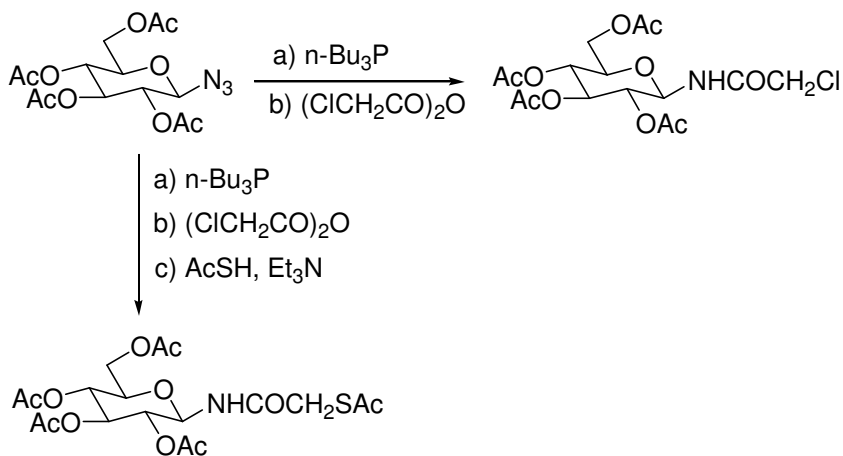
The main problems observed in the reduction of glycosylazides are principally inter- or intramolecular migration of an O-acetyl group, hydrolysis, and anomerization. The severity of these problems is dependent on the protecting groups on the sugar, the catalyst used for hydrogenation, the solvent system employed and the size of the carbohydrate moiety. In order to avoid glycosyl anomerization, reduction of glycosyl azides has been carried out in the presence of symmetric or mixed anhydrides of the β -carboxylic acid of aspartic acid derivatives.¹⁵ However, α - and β -mixtures were obtained in this case as well.

II. Via Glycosyl Azides

Another commonly employed strategy to synthesize β -N glycosidic bonds is using glycosyl azides which can be easily prepared in high stereoselectivity and high yields (80-95%).^{16,17} The starting materials for the synthesis of glycosyl azides are typically halides, acetates, oxazolines or glycols. Using a glycosyl acetate, oxazoline, or glycol as a precursor provides only β -glycosyl azide, while using β - or α -glycosyl halides can provide both α - or β -glycosyl azides, respectively.¹⁸

The Santoyo-Gonzalez group has developed an efficient one-pot synthesis of chloroacetyl and S-acetylmercaptoacetyl N-glycosides from glycosyl azides. In both the procedures they have carried out a mild reduction of the azido group using $n\text{-Bu}_3\text{P}$ and 1, 3-propanedithiol as reducing reagents, respectively (Scheme 2).¹⁹

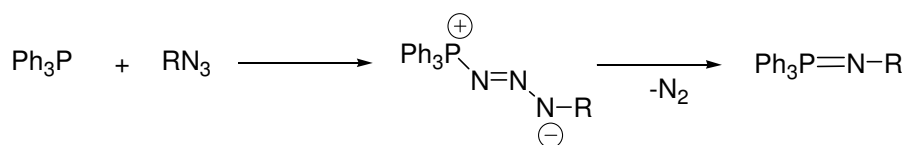
Scheme 2



III. Via Glycosyl Phosphorimines: the Staudinger Reaction

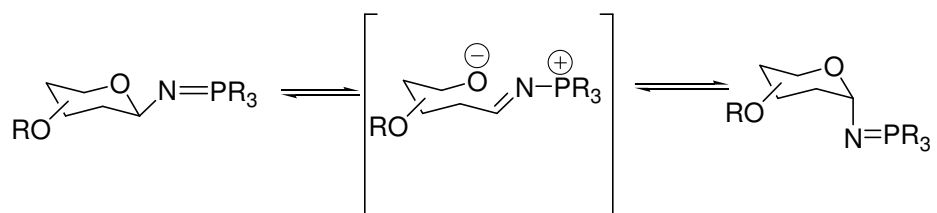
The classical Staudinger reaction is a two step process involving the initial electrophilic addition of an azide to a trialkyl or triaryl phosphine followed by nitrogen elimination from the intermediate phosphazide to give the iminophosphorane.^{20, 21} The addition is not hindered by the substituents at phosphorus, and its rate is controlled by the inductive influence of the substituents and by the azide electrophilicity. Usually, the imination proceeds smoothly, almost quantitatively, without the formation of any side products.

Scheme 3



In the reaction of a glycosylazide with a trialkyl/aryl phosphine the glycosylphosphazene intermediate is known to anomerize via an open-chain structure (Scheme 4).²²

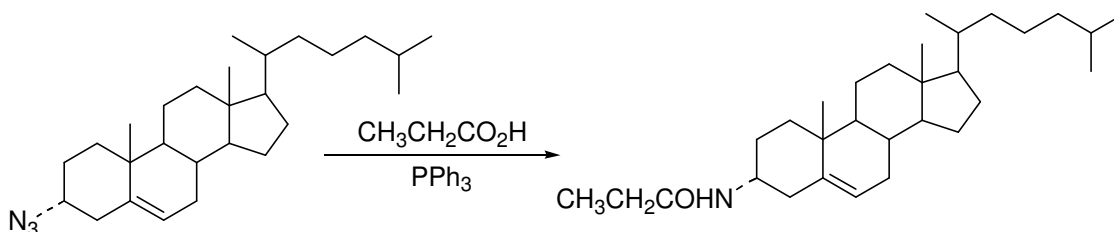
Scheme 4



There have been several applications of the Staudinger reaction in the recent past. Garcia et al. performed a one-pot reaction of carboxylic acids with aryl or alkyl

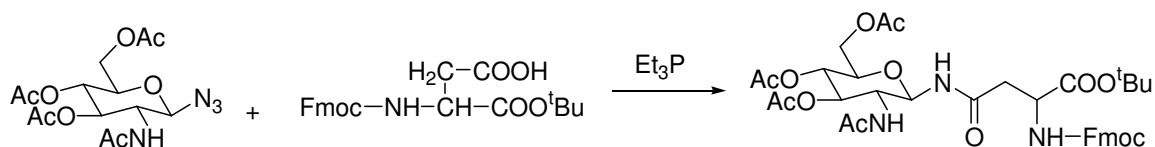
azides and Ph_3P under non-acidic conditions without employing expensive additional reagents (Scheme 5).²³

Scheme 5



Inazu group performed the coupling reaction of glycosyl azide with N^α Fmoc-L-aspartic acid α -monoester in the presence of Et_3P in CH_2Cl_2 (Scheme 6).²⁴

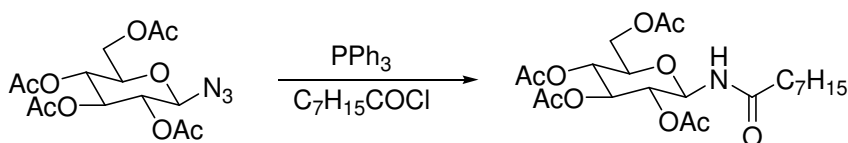
Scheme 6



There were several drawbacks of this reaction. It required reactive phosphines (Et_3P), was time consuming (several hours) and the yields were strongly dependent on the structure of the glycosyl azide (from 77% with GlcNAc to 23% for Glc derivatives). In order to overcome these problems a modified Staudinger reaction was proposed by the Boullanger group.²⁵ They developed optimum conditions for the coupling reaction of glycosyl azides and acyl chlorides using triphenylphosphine which

although has a lower reactivity but is stable to oxidation and hydrolysis and is easier to handle than non-aromatic phosphines. This was an efficient methodology to prepare glycosylamides from glycosyl azides in very good yield and high anomeric stereoselectivity (Scheme 7).

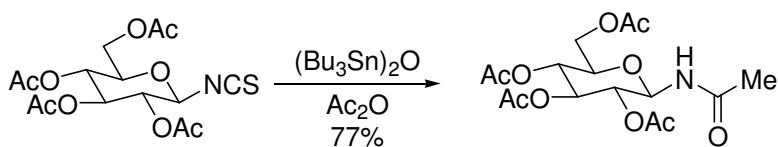
Scheme 7



Other Methodologies

The Gonzalez group has developed a simple, efficient and one-pot procedure for the preparation of glycopyranosylamines and their N-acyl derivatives from glycopyranosyl isothiocyanates using bis (tributyltin) oxide as the reductive reagent (Scheme 9).²⁶

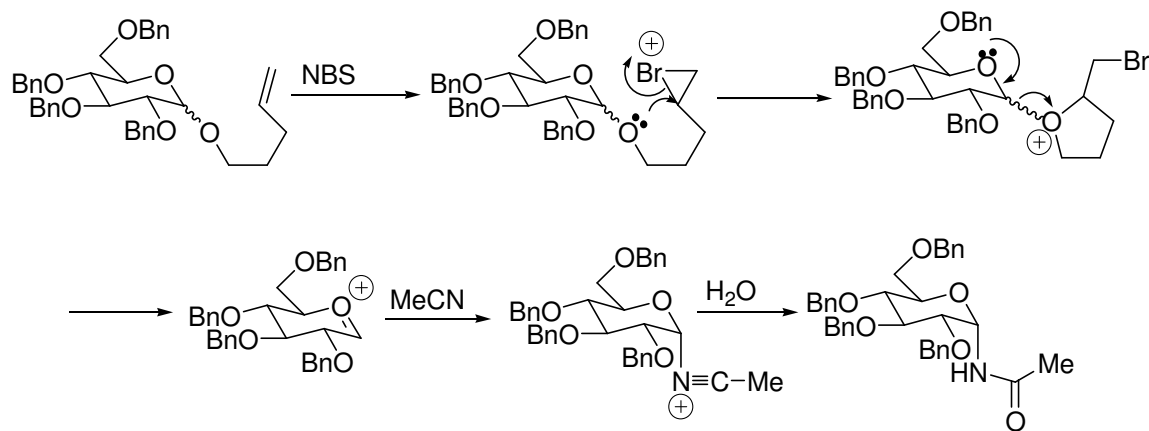
Scheme 8



One of the strategies to stereospecifically create the α -D-glucopyranosylacetoneitrilium was developed by Ratcliffe et al.²⁷ They utilized the N-bromosuccinimide (NBS) to cause the cleavage of the glycosidic acetal in pent-4-enyl glucopyranosides leading to

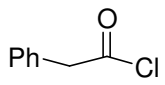
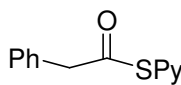
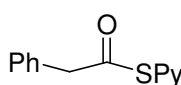
the formation of α -N-acetylglycopyranosylamine via a cyclic oxocarbenium ion (Scheme 10).

Scheme 9

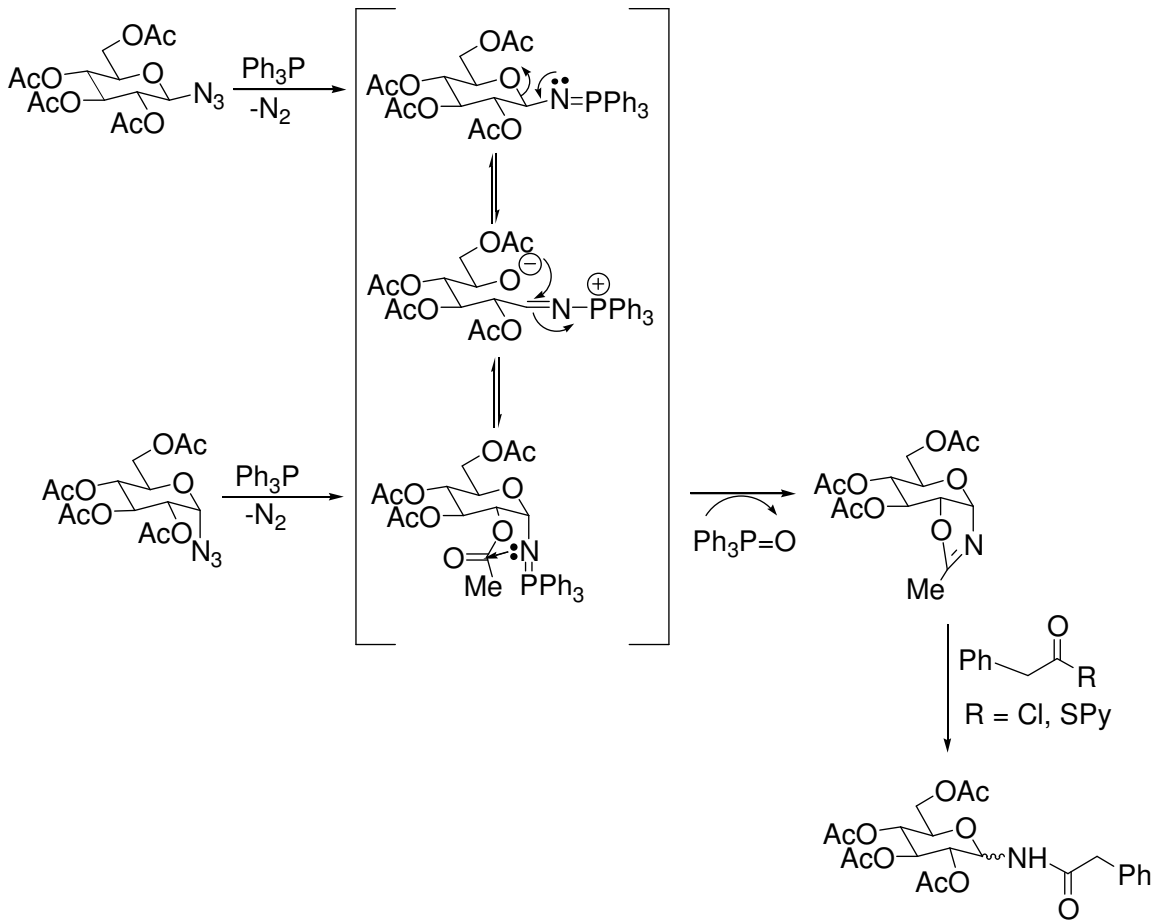


The DeShong group has also used modified Staudinger reaction to perform a stereoselective synthesis of an α -N-linked glycopeptide from 1-azidoglycopyranosyl derivatives.²⁸ In this methodology the stereochemistry of the intermediate isoxazoline controls the stereochemistry at the newly formed anomeric centre (Scheme 10). Treatment of either β -azide or α -azide with Ph₃P in refluxing dichloroethane gave isoxazoline which was then acylated with a variety of reagents to yield the α -adduct in a highly stereoselective process (Table 1).

Table 1. Coupling reactions using modified Staudinger methodology.

| Entry | Reagent | Equiv. | Additive | Temp (°C) | Yield (%) | α/β |
|-------|---|--------|--------------------------------------|-----------|-----------|----------------|
| 1. |  | 4 | - | 83 | 51 | > 19/1 |
| 2. |  | 1.3 | - | 83 | 67 | 5/1 |
| 3. |  | 1.3 | CuCl ₂ ·2H ₂ O | 30 | 80 | 98/2 |

Scheme 10



Thiopyridyl coupling reactions were performed by Fehmi Damkaci using di- and triglycosyl azides as well to prove the generality of the methodology.

The goal of my project was to utilize the Staudinger methodology developed in our group and synthesize α - and β -linked oligosaccharides which could be used to tether to gold films and nanoparticles and characterize the resulting films and particles. Gold nanoparticles functionalized with oligosaccharides are of fundamental importance in controlling the mesoscopic properties of new materials and in developing new tools for nanofabrication. Also, our aim was to attach the

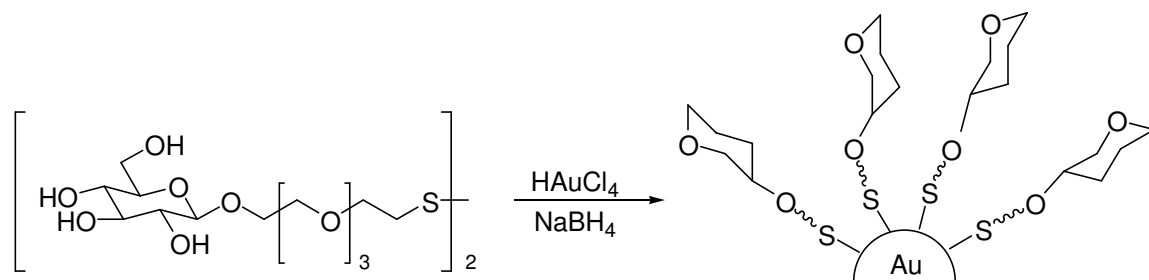
oligosaccharides to gold films and study the formation of self-assembled monolayers (SAMs) on gold films.

Oligosaccharide Functionalized Gold Nanoparticles

Metal nanoparticles coupled with biomolecules have generated a lot of interest recently because the resulting materials have applications in biological systems. The biomolecules most commonly used to date are DNA or protein and very few examples of carbohydrates have been reported.^{29,30,31}

A methodology which allows for the preparation of glyconanoparticles with biologically significant oligosaccharides as well as with differing carbohydrate density has been developed by Barrientos et al.³² Their approach provides water soluble monolayer protected gold nanoclusters. The particles are prepared by in situ reduction of a gold salt in the presence of excess of the corresponding thiol-derivatised neoglycoconjugate. The mild conditions and moderate reducing agents used in this process are compatible with a wide range of ligand functionalities. The size of the nanoparticle can be controlled through the stoichiometry of the metal salt to the capping ligand (Scheme 11).

Scheme 11



They functionalized the gold nanoparticles with the monosaccharide glucose, disaccharide lactose and maltose or trisaccharide Lewis X antigen and did the characterization using ^1H NMR, UV, IR and TEM; which showed clear differences related to the sugar protected clusters. These glyconanoparticles provide a glycocalyx like surface with a globular shape and well defined structure which makes them a promising tool for biological and biotechnological applications. Also, size and pattern arrangement of the metallic cluster could be controlled by using this methodology.

The Bernad and Penadés group has also reported the first application of glyconanoparticles as antiadhesion tools against metastasis progression.³³ They have found that short *ex vivo* preincubation of tumoral cells with lactose-glyconanoparticles is enough to substantially inhibit lung metastasis (up to 70%) although the process is not capable of eradicating the phenomenon.

Lin et al. have developed a novel method of labeling specific proteins on the cell-surface using carbohydrate conjugated nanoparticles.³⁴ They have shown that mannose encapsulated Au nanoparticles have a strong and selective binding to bacterial Type 1 pili and can be used as efficient labeling probes.

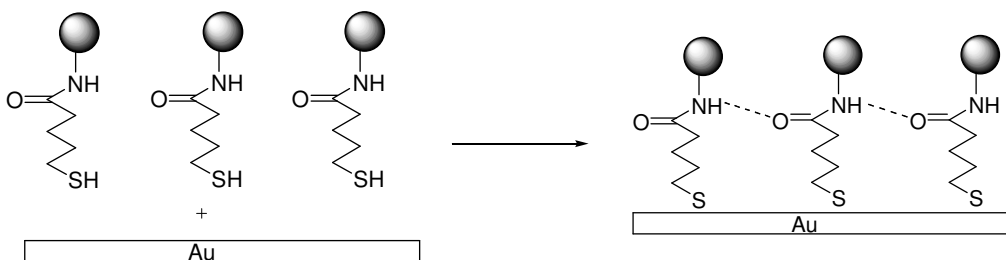
The Chia-Chun Chen group has explored the multivalent interactions between the carbohydrate encapsulated gold nanoparticles and lectins.³⁵ The lectin they used was concanavalin A which binds specifically to mannose and glucopyranosides³⁶ and have shown that the mannose-Au nanoparticle and Con A interactions are affected by the nanoparticles size and the linker of the mannose ligands.

Surface modification of metal nanoparticles with organic molecules have application in the design of nanostructured materials.³⁷

Synthesis and Characterization of Self-Assembled Monolayers (SAMs). Self assembled monolayers (SAMs) are ordered molecular assemblies formed by the adsorption of an active surfactant on a solid surface.³⁸ There are different kinds of self assembled monolayers, the most widely studied being the monolayers of alkane thiolates on silver, copper and gold surfaces.³⁹

Sulfur compounds have a strong affinity to transition metal surfaces probably because of the possibility to form multiple bonds with the surface metal clusters.^{40,41,42,43} It has been found that organosulfur compounds also coordinate very strongly to silver.⁴⁴

Ordered monolayers are formed by a strong chemical bond formation (chemisorption) of molecules with the surface and due to group specific intermolecular or chain-chain interactions (H-bonding).



The alkanethiolates can form monolayers on both gold and silver surfaces. SAMs derived from unfunctionalized alkanethiols $\text{HS}-(\text{CH}_2)_n\text{CH}_3$ are easily prepared by the reaction of solutions or vapors of these compounds with gold.^{45, 46, 47, 48} The polymethylene chains in these SAMs are predominantly trans-extended when $n > 10$.

The two dimensional structure of SAMs can be controlled by introduction of specific interchain interactions. Dipole-dipole or hydrogen bonding interactions may lead to an enhancement of packing and ordering and these might be envisioned by introducing sulfone or amide groups into the alkyl chain.

The Rotello group has observed inter and intramonolayer H-bonding in amide functionalized SAMs on gold nanoparticles.⁴⁹ They have shown that the ability of the amide to participate in hydrogen-bonding gets reduced as the amide is moved further out along the monolayer chain. This is due to the increasing disorder of the monolayer as the distance from the core increases, making intramonolayer interactions more entropically disfavored. Also, hydrogen-bonding is reduced if the amide functionality is too close to the gold core. This decrease in efficiency of hydrogen bonding arises due to steric factors because of the proximity of the amide to the monolayer protected surface. The greatest hydrogen-bonding was observed for the compound in which the amide was 3-4 carbons away from the core. Fritz et al. have performed surface characterization of thiol terminated oligosaccharides adsorbed on a gold surface.⁵⁰ They have synthesized a thiol terminated hexasaccharide, protected with acetyl groups which they have used to form self-assembled monolayers (SAMs) onto gold surfaces. SAMs have been characterized using a variety of techniques. XAS (X-ray absorption spectroscopy), XPS (X-ray photoemission spectroscopy), FT-IR analysis, contact angle and surface plasmon resonance are a few techniques which have been used to characterize the chemical interaction between gold surfaces and self assembled monolayers.^{51,52,53}

SAMs provide a good opportunity to enhance the basic understanding of self-organization and interfacial phenomena. SAMs of functionalized alkanethiols on gold substrates are the most commonly used templates for the chemical construction of advanced electronic devices and sensors.^{54,55}

Goals of My Research

The goal of my research was to synthesize oligosaccharides which could be used to functionalize gold nanoparticles and form self assembled monolayers on gold films. It is well known that gold forms very strong chemical bonds with thiols and disulfides, so one of our goals was to synthesize α - and β -linked sugars with a thiol or a disulfide attachment using modified Staudinger reaction which has been developed in our laboratory by Fehmi Damkaci.

The second goal was to attach the oligosaccharides to gold films and to characterize the resulting gold films.

The third goal was the synthesis of gold nanoparticles and the attachment of these oligosaccharides to these nanoparticles. The basis for doing this was to be able to use these carbohydrate-attached gold nanoparticles as labeling probes in biological systems and also in biological assays. As mentioned in my discussion above there are examples of sugar functionalized nanoparticles in the literature which have been used as an efficient labeling probe but so far their application in biological assays has not been explored.

Results and Discussion

Synthesis of Glucopyranosylamides

It is well known that thiols and disulfides have a strong affinity for gold surfaces.⁵⁶

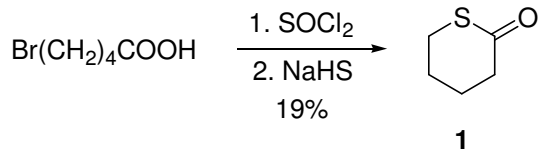
Our goal was to synthesize oligosaccharides with a thiolated or a disulfide side chain which could be used to functionalize gold films and gold nanoparticles.

In order to synthesize an oligosaccharide with a thiol group at the end, the first step was the synthesis of a 5- or 6-membered thiolactone which would couple with peracetylated glucose β -azide under the modified Staudinger reaction conditions to give the desired sugar with an amide linkage and thiolated side chain.

In our lab Fehmi Damkaci has worked on the modified Staudinger reaction.²⁶ He found that the reaction is highly stereoselective and proceeds via the formation of an isoxazoline intermediate which then undergoes the coupling reaction. The α - and β -linked azides form the respective α - and β -phosphorimine intermediate which can anomerize via the open chain form ultimately leading to the formation of the α -linked isoxazoline. This isoxazoline intermediate then undergoes coupling reaction with the various substrates to give the α -linked amide (Scheme 8).

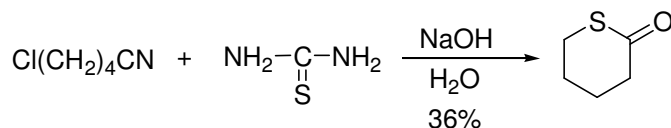
Two different methods were tried to synthesize the thiolactone. In the first method 5-bromovaleric acid was treated with sodium hydrogen chalcogenide containing tetrabutylammonium hydrogen sulphate as the phase transfer agent. A very low yield of 19% was obtained for this reaction (Scheme 12).

Scheme 12



The second approach to synthesize the thiolactone involved treating 5-chlorovaleronitrile, with thiourea and water (Scheme 13).

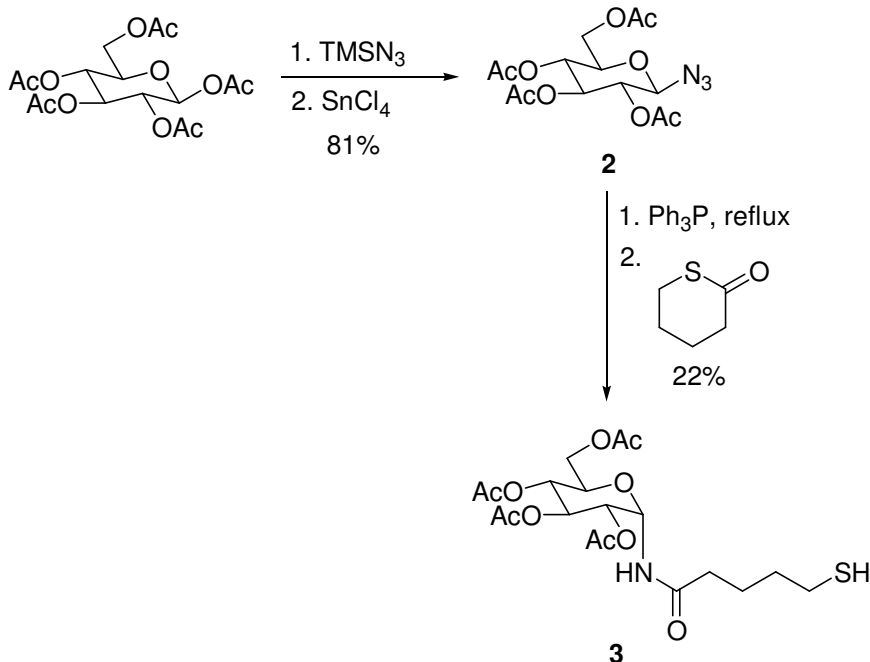
Scheme 13



Peracetylated glucose β -azide, the coupling partner for the thiolactone was synthesized from the corresponding glucose octaacetate in a high yield (81%) (Scheme 14).

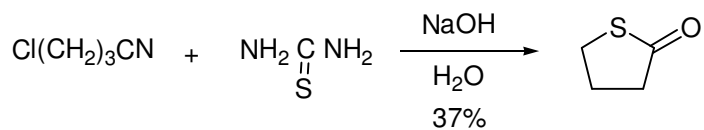
Treatment of peracetylated glucose β -azide with Ph_3P in refluxing 1, 2-dichloroethane in the presence of 4 Å molecular sieves for 15 h gave isoxazoline as an intermediate which was characterized by graduate student Fehmi Damkaci in our lab. The isoxazoline intermediate then coupled with the thiolactone to give the open chain thiol form in 23% yield (Scheme 14).

Scheme 14



At this point it was thought that the 5-membered thiolactone might be a better coupling partner for reaction with peracetylated glucose β -azide because it should be more reactive than the 6-membered thiolactone. The synthesis of the 5-membered thiolactone by treating γ -chlorobutyronitrile with thiourea in the presence of NaOH was performed (Scheme 15).

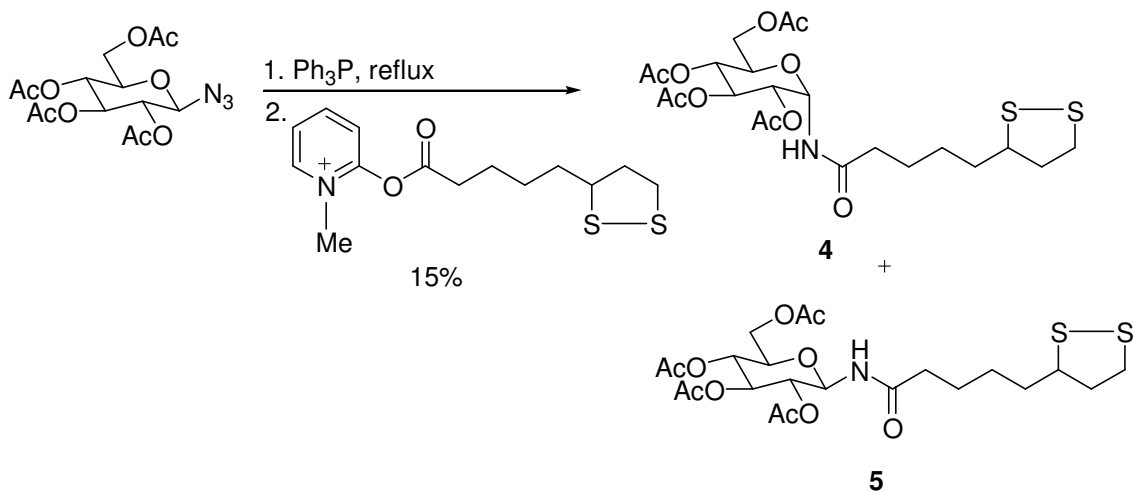
Scheme 15



A yield of 37% was obtained on this reaction but the final coupling with the azide was unsuccessful.

Subsequent studies in the group by Juhee Park have provided an alternative method to synthesize glucopyranosylamide **3** in better yields. Since the thiolactones were tedious to make and were very unstable, synthesis of oligosaccharides with side chains having the disulfide group was attempted by employing thioctic acid (lipoic acid) and derivatives of thioctic acid as the coupling partner with the glucose β -azide. The other substrate that was tried out as the coupling partner was 2-fluoro-1-methylpyridinium-p-toluene sulfonate (FMPPTS). The reaction using this however, gave a very low yield, in addition a mixture of the α - and β - products was obtained (Scheme 16).

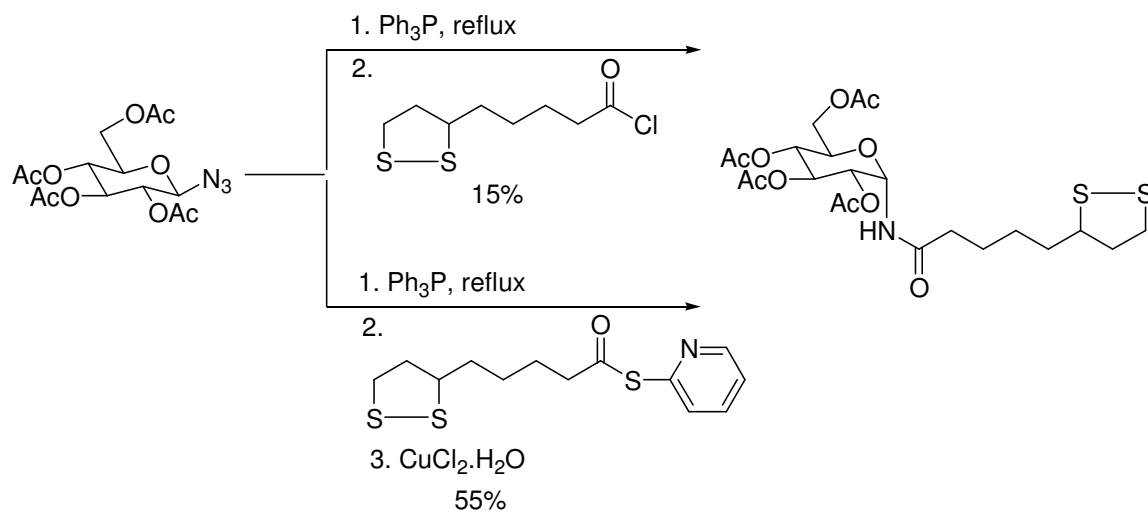
Scheme 16



The coupling reaction of peracetylated glucose β -azide with thioctoyl chloride was attempted but the yield was very low. The coupling reaction worked best when it was performed with thioctic ester (Scheme 17). The addition of Cu (II) chloride salts in this particular reaction causes an enhancement in the yield of the reaction presumably

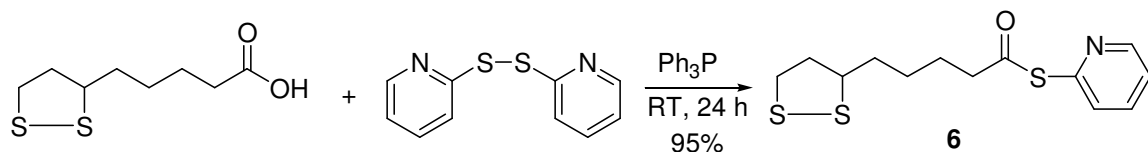
because the coordination of copper to the nitrogen of the pyridyl moiety increases the electrophilicity of the ester.²⁶

Scheme 17



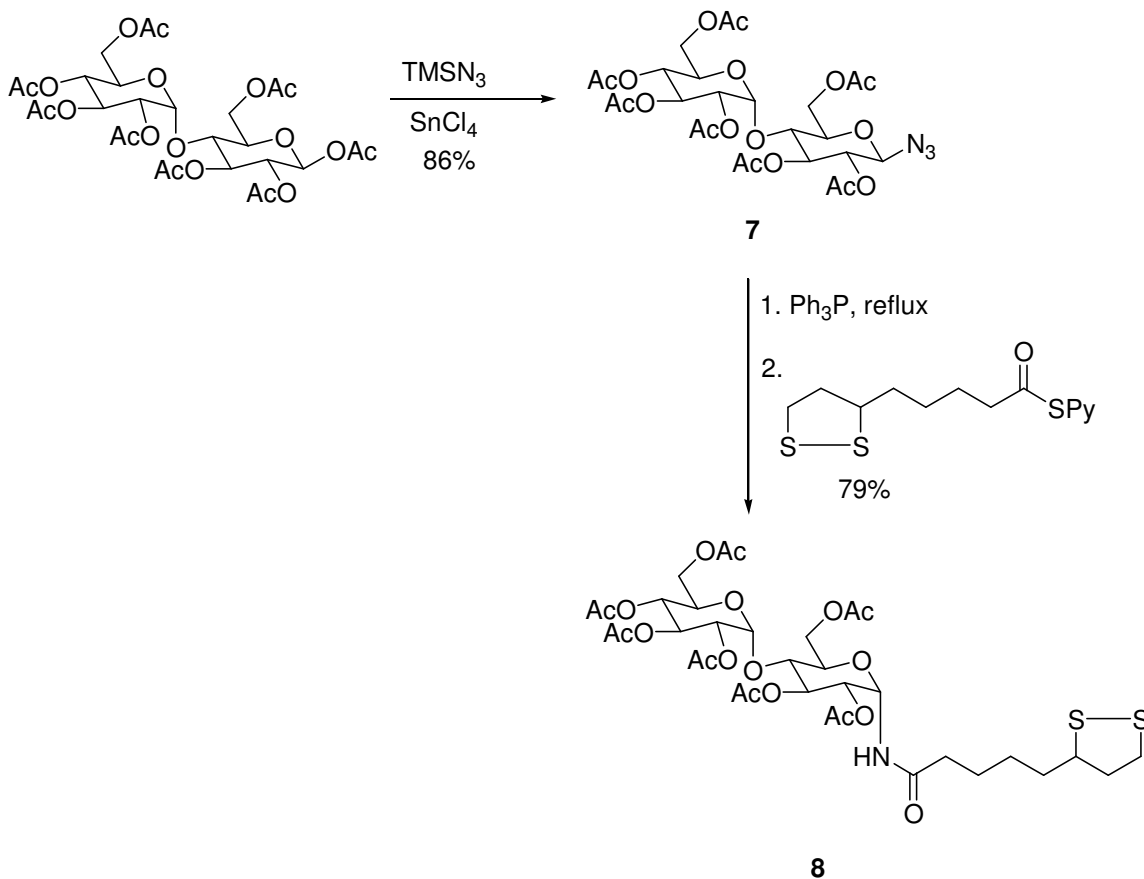
The thioctic ester utilized in the coupling reaction was prepared in high yield (95%) by the coupling of thioctic acid with dithiodipyridine (Scheme 18).

Scheme 18



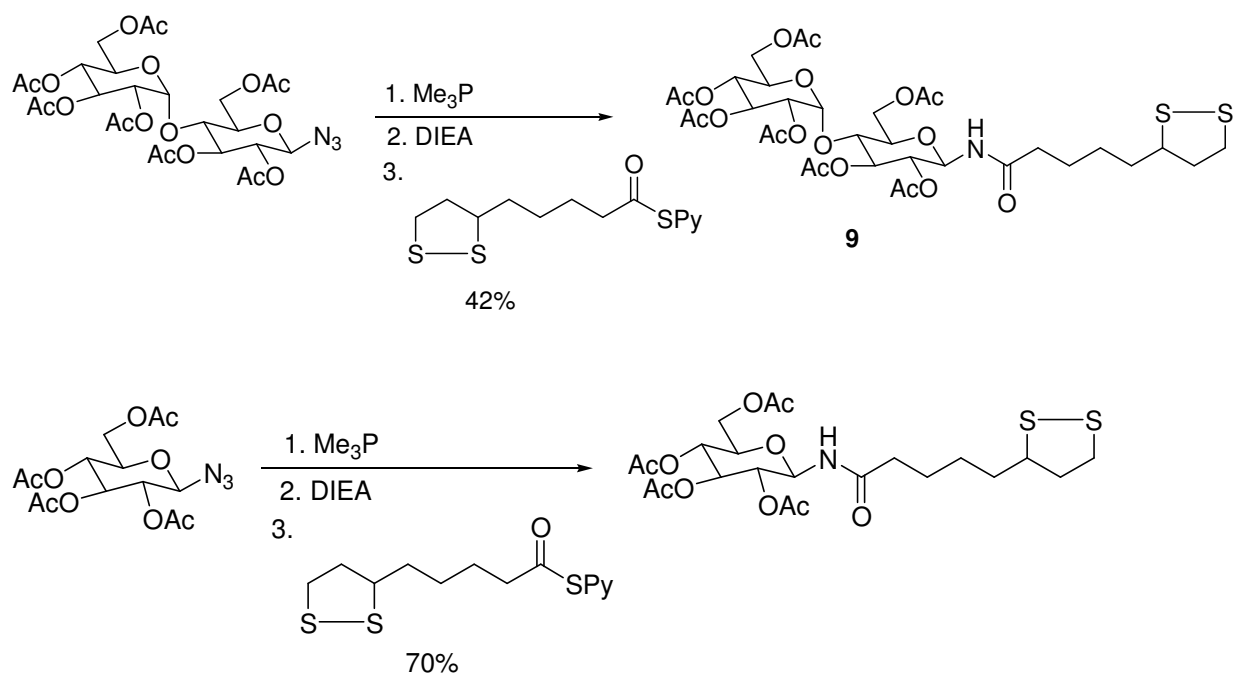
In order to check the generality of this methodology similar reactions were performed with the disaccharide maltose (Scheme 19). The reactions with maltose worked in comparable yields.

Scheme 19



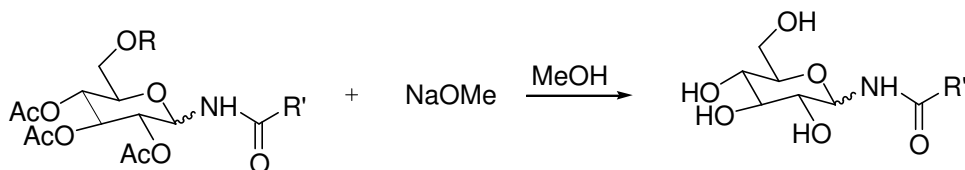
In order to determine whether there would be any difference between the α - and the β - linked oligosaccharides when they are bound to the gold surface the synthesis of β -linked disulfide side chain in the glucose and maltose sugars was performed (Scheme 20).

Scheme 20



Finally, hydroxylations were performed to convert all the acetates into hydroxyl groups (Table 2). The hydroxylated sugars were used for functionalization of gold nanoparticles and gold films.

Table 2. Hydroxylation Reaction for oligosaccharides with thiolated and disulfide side chains.



| Starting Material | Product | Yield (%) |
|----------------------------------|---|-----------|
| α -Glu-OAc-SH | α -Glu-OH-SH (10) | 75 |
| β -Glu-OAc-S ₂ | β -Glu-OH-S ₂ (11) | 68 |
| β -Mal-OAc-S ₂ | β -Mal-OH-S ₂ (12) | 30 |
| α -Glu-OAc-S ₂ | α -Glu-OH-S ₂ (13) | 57 |
| α -Mal-OAc-S ₂ | α -Mal-OH-S ₂ (14) | 40 |

Gold Films

Oligosaccharides were tethered onto gold films and several experiments were performed for their characterization like FT-IR, Scanned probe microscopy, XPS, contact angle measurements. Self assembled monolayer formation was observed for the hydroxylated oligosaccharides and multilayer formation was observed in the case of the α -linked hydroxylated oligosaccharide with a thiol side chain. The FT-IR studies were performed in collaboration with Drs. Aric Opdahl and Michael Tarlov at NIST.

FT-IR of oligosaccharides with thiolated side chain

FT-IR was performed on three oligosaccharide samples: α -glu-OH-SH, α -glu-OAc-SH and α -glu-OH-CH₃ adsorbed on gold film. The gold films were soaked in the

oligosaccharide solutions for 2 h and then resoaked for 20 h. In the case of α -glu-OAc-CH₃, a carbonyl peak at 1754 cm⁻¹ was observed for both the 2 h and 20 h spectra (Fig. 3). This peak is very weak in intensity and it arose presumably due to physisorption of the oligosaccharide on the gold surface. No chemical bonds are expected between this oligosaccharide and the gold film due to the absence of thiol group.

In the case of α -glu-OAc-SH, a peak characteristic for esters was observed at 1765 cm⁻¹ for both the 2 h and 20 h spectra (Fig. 4). The amide peak is not observed because it is believed that amides lie parallel to the gold surface and based on metal-surface selection rule only those modes which have vibrational dipole moments with components perpendicular to the metal surface have measurable intensities.⁵⁷

The results with α -glu-OH-SH were the most intriguing. When the film was soaked for 2 h there was no significant peak for either amides or esters but after 20 h there is a prominent increase in the amide peak at 1643 cm⁻¹ (Fig. 5). This suggests evidence for intermolecular H-bonding between the hydroxyls of one oligosaccharide with the carbonyl of another oligosaccharide. There is also evidence for the amide peak in α -helices to be about 1650 cm⁻¹ and this is due to the strong hydrogen bonded network present in these helices.⁵⁸

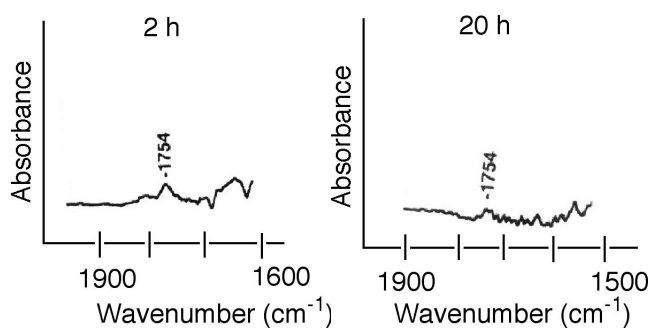


Figure 3. FT-IR of α -glu-OAc-CH₃ at 2 h and 20 h.

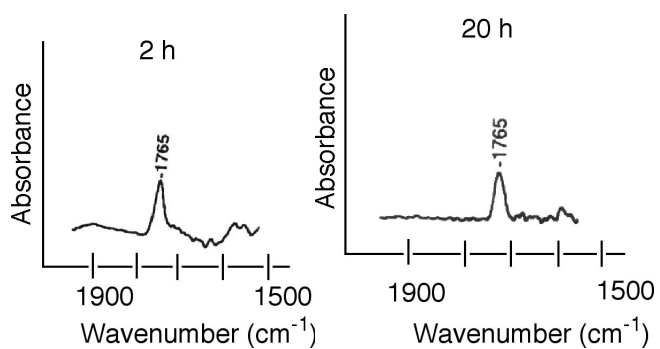
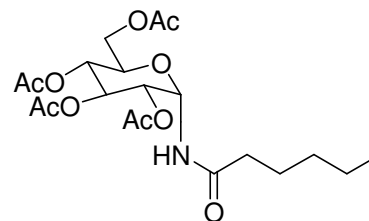


Figure 4. FT-IR of α -glu-OAc-SH at 2 h and 20 h

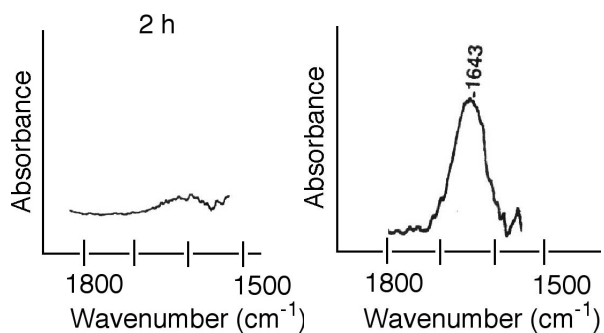
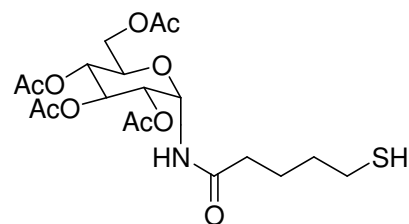
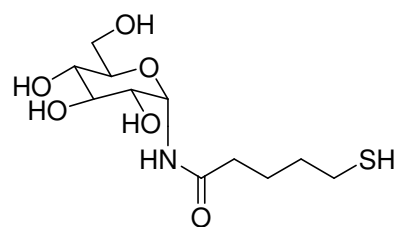


Figure 5. FT-IR of α -glu-OH-SH at 2 h and 20 h.



FT-IR of oligosaccharides with disulfide side chains

FT-IR was performed on hydroxylated oligosaccharides having disulfide side chains. In the case of α -glu-OH-S₂, a different trend was observed from α -glu-OH-SH. There was no notable growing in of the amide peak after the films were soaked for 20 h (Fig. 6).

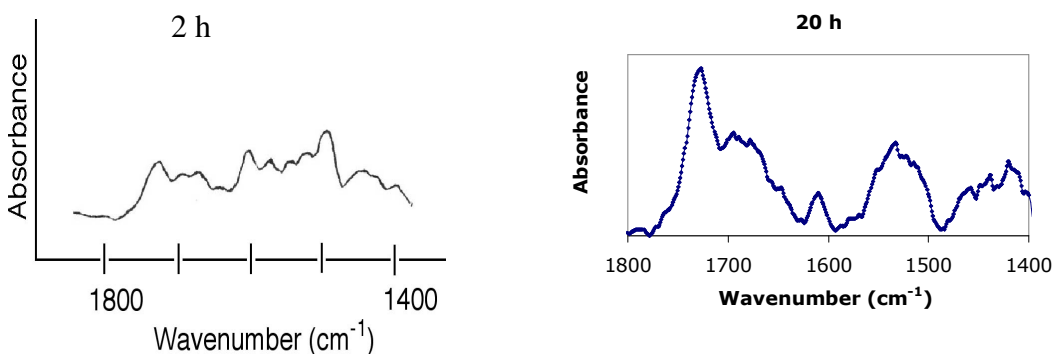


Figure 6. FT-IR of α -glu-OH-S₂ at 2 h and 20 h.

Similar results were obtained in case of the β -linked oligosaccharides. The spectra for the 2 h and 20 h runs were similar and there was no significant increase in the amide peak (Fig. 7). However, differences were observed in the spectra of α - and β -linked hydroxylated oligosaccharides with disulfide side chain (Fig. 6-7). The α -linked hydroxylated glucose sugar showed a peak at 1730 cm⁻¹ which is not observed in case of the β -linked hydroxylated oligosaccharide. This peak might be attributed to the blue shift in the amide peak.⁵⁹

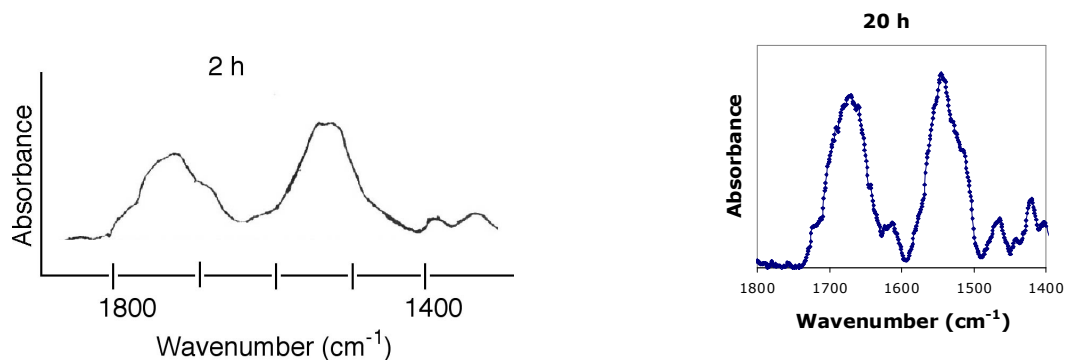


Figure 7. FT-IR of β -glu-OH-S₂ at 2 h and 20 h.

Scanned Probe Microscopy of Glucosylated Gold films. The morphology of a representative set of glucose SAMs on gold were examined by atomic force microscopy (AFM) for incubation times of 2 and 20 h. For glucosylamides **10** and **13**, after 2 h of deposition, monolayers were observed with approximately 10% and 25% of a bilayer present, respectively. From nanografting of dodecanethiol and hexadecanethiol into the glucosylamide **10** and **13**, the monolayer thicknesses were estimated to be ~ 1 nm for each. For the acetate functionalized glucosylamide **4** however, monolayer formation was never observed under the identical deposition conditions. The acetylated glucosylamide **4** was found to form only multilayered films with thickness on the order of ~ 5 nm, suggesting that the acetylated glucosylamides readily aggregate either before or during deposition. For deposition of each of these compounds after 20 h the glucose monothiol and disulfide films showed clean smooth films on the Au surface with little to no evidence of a bilayer,

while the acetylated glucosylamide **4** was unchanged in its observed morphology and film thickness. The packing density appeared to be higher for the glucose thiol than for the glucose disulfide, which was consistent with the larger footprint of the disulfide on the Au surface. This was noted as larger graininess in the disulfide images at 20 h in comparison to the smooth films found for the glucose thiol monolayers.

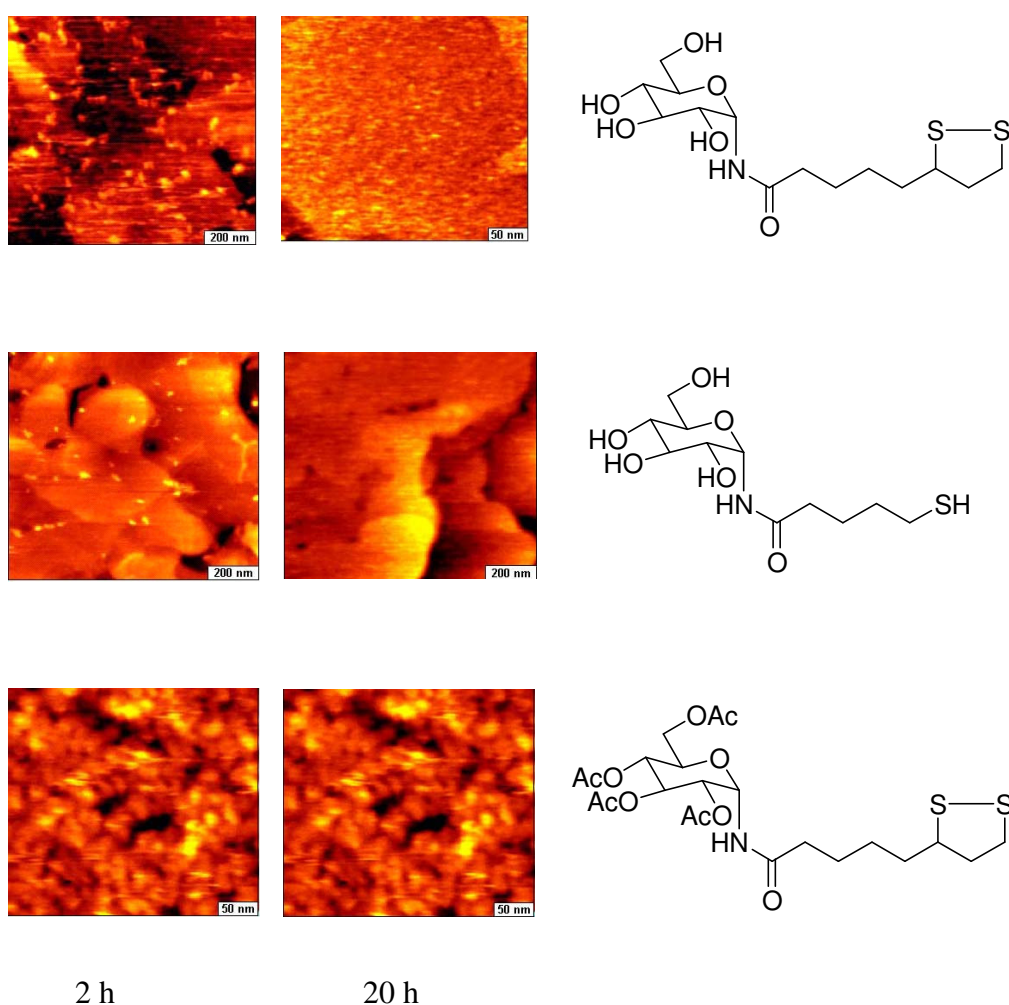
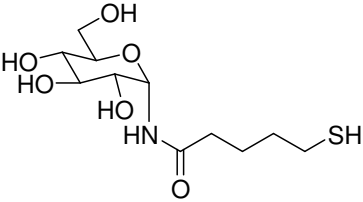
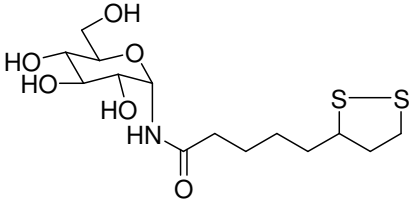


Figure 8. Comparison of oligosaccharide SAMs after 2 and 20 h immersion.

X-Ray Photoelectron Spectroscopy of Glucosylated Gold films. Films prepared from glycosylamides **10** and **13** were studied by X-ray photoelectron spectroscopy (XPS) and the results are summarized in Table 3.

Table 3. Results of XPS Analysis of Monolayers on Gold.

| Glycopyranosylamides | S/Au | N/Au |
|--|------|------|
|  | 0.06 | 0.09 |
|  | 0.06 | 0.09 |

The S/Au ratio is indicative of surface coverage by the thiol components of the SAM. There is precedence in literature that a S/Au ratio of 0.08 indicates a highly organized, self-assembled monolayer coverage for a well-ordered self-assembled monolayer of butanethiol.⁶⁰ It was observed that in most cases irrespective of the oligosaccharide having a thiolated side chain or a disulfide side chain the S/Au, N/Au, O/Au ratios are higher for the hydroxylated oligosaccharide as compared to the acetylated oligosaccharide and the value for S/Au is close to 0.08 for the hydroxylated oligosaccharides which indicates that the hydroxylated oligosaccharides might be forming an ordered monolayer. The mechanism we propose for the ordered

monolayers in case of hydroxylated oligosaccharides is possibly due to hydrogen bonding between amide carbonyl of one chain and nitrogen of another chain (Fig. 9).

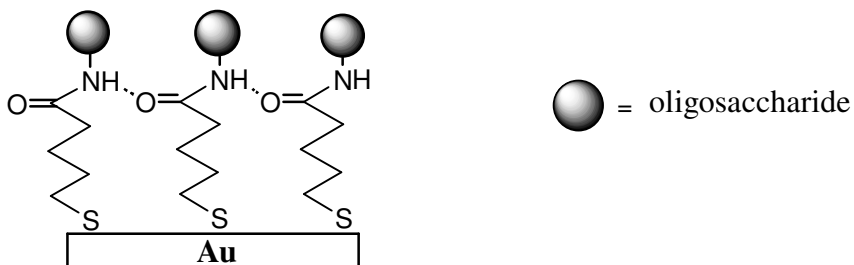


Figure 9. Proposed mechanism for ordered monolayer formation.

In the case of oligosaccharides having disulfide as the side chain the footprint on gold is considerably larger than in the case of oligosaccharides with thiolated side chains. The presence of the acetate groups adds to the steric bulk of the molecule and therefore there is a smaller number of these compounds on the same surface area of gold causing the S/Au, O/Au and N/Au values to be lower for them.

There is a consistent trend in the S/Au ratios across the disulfide series of oligosaccharides. The values are considerably lower for the acetylated oligosaccharides than for the hydroxylated oligosaccharides. A reversed trend was observed for α -glu-SH in which case the S/Au ratio is higher for the acetylated oligosaccharides (Fig. 10)

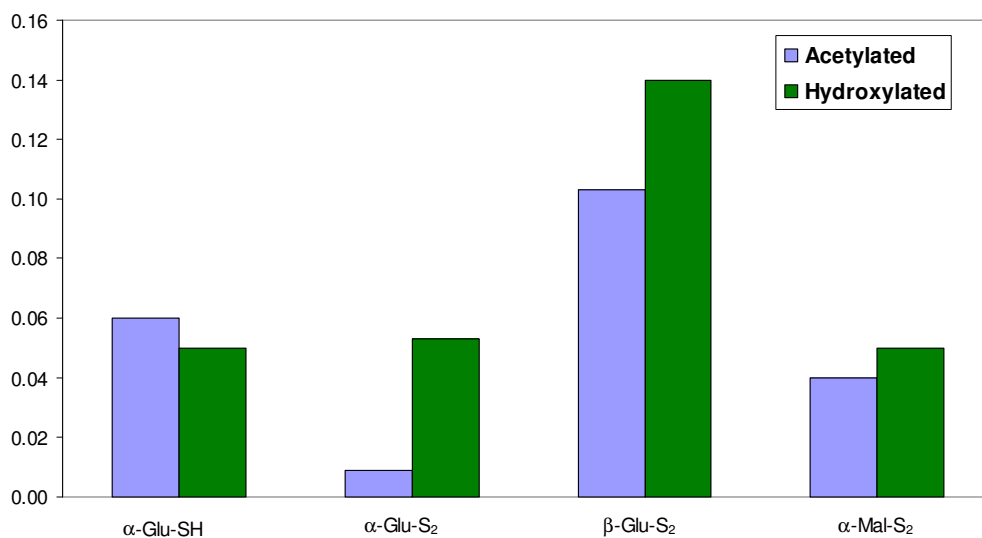


Figure 10. S/Au ratios for acetylated and hydroxylated oligosaccharides.

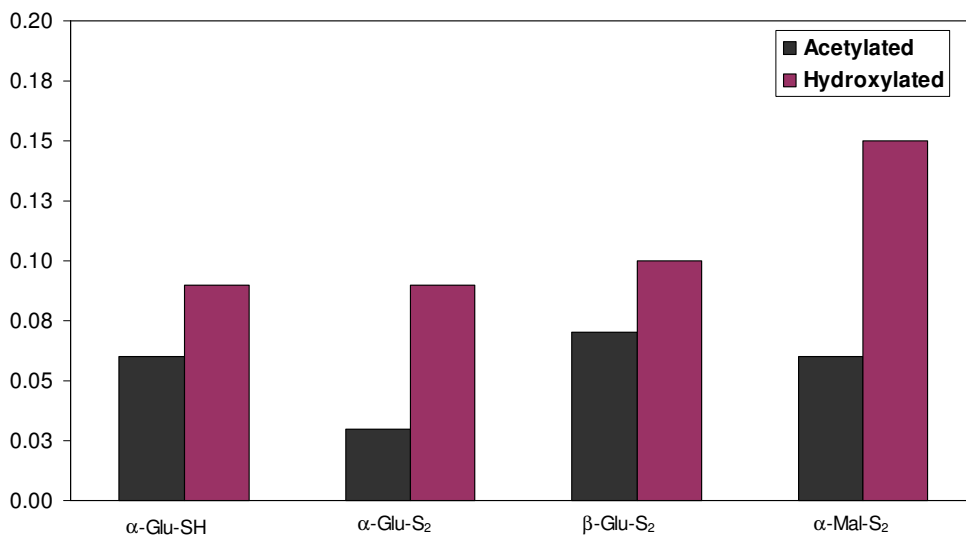


Figure 11. N/Au ratios for acetylated and hydroxylated oligosaccharides.

The hydrogen bonded nitrogen occurs at a higher binding energy than the non-hydrogen bonded nitrogen.⁶¹ Only one kind of nitrogen was observed for β -glu-OAc-S₂ and α -glu-OAc-S₂. There is a more prominent H-bonded nitrogen for the

hydroxylated oligosaccharides which is as expected because there is not much steric hinderance in the case of the hydroxylated oligosaccharides which allows them to come close together and hydrogen bonding is possible between the carbonyl of one oligosaccharide and the hydroxyls of the second oligosaccharide (Fig. 12).

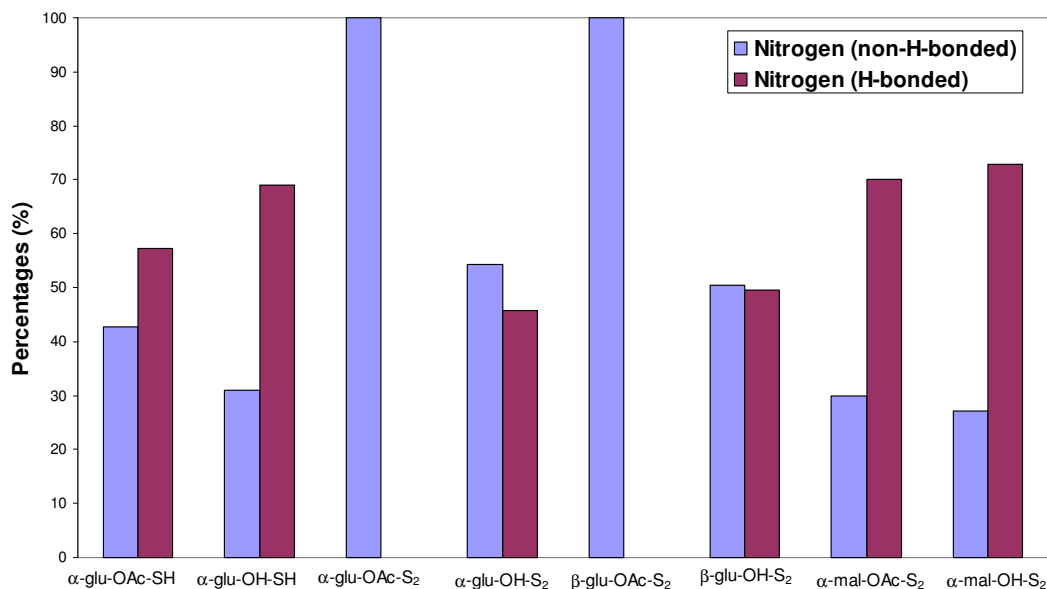


Figure 12. Comparison of nitrogen (non-H-bonded) and nitrogen (H-bonded) for acetylated and hydroxylated oligosaccharides.

Contact Angle Measurements

The underlying principle behind this experiment is that more hydrophobic samples have a higher contact angle because on a hydrophobic surface the drop of water sits like a sphere and does not spread out. It was observed that the contact angles for the acetylated oligosaccharides were higher than for the hydroxylated oligosaccharides which is as expected because the acetylated oligosaccharides are more hydrophobic

as compared to the hydroxylated oligosaccharides which are hydrophilic due to the presence of hydroxyl groups (Table 4).

Table 4. Contact angles for oligosaccharides.

| Oligosaccharides | Contact Angles(°) |
|----------------------------------|-------------------|
| α -Glu-OAc-SH | 36 |
| α -Glu-OH-SH | 35 |
| α -Glu-OAc-S ₂ | 65 |
| α -Glu-OH-S ₂ | 32 |
| α -Mal-OAc-S ₂ | 45 |
| α -Mal-OH-S ₂ | 24 |
| Blank Au | 92 |

Gold Nanoparticles

Au nanoparticles of 5 nm diameter were prepared and attached to oligosaccharides having thiol and disulfide side chains and the method of characterization used was transmission electron microscopy (TEM). A TEM experiment was performed which involved bare Au nanoparticles in a solution of CH₂Cl₂. It was found that these particles were randomly dispersed (Fig. 13). The size distribution for these nanoparticles was 3-7.

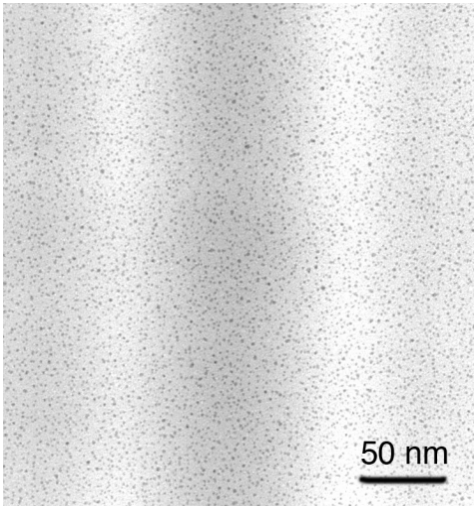


Figure 13. TEM of Au nanoparticles prior to surface functionalization.

In another experiment gold nanoparticles were added to a solution of α -glu-OH-SH and these TEM images showed clustering of the gold nanoparticles. There is presence of hydrogen-bonding between the hydroxylated oligosaccharides and since they are bound to nanoparticles they cause aggregation of gold nanoparticles (Fig.14).

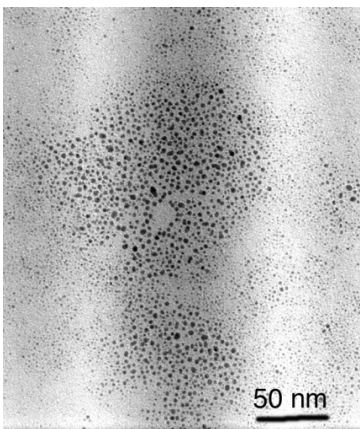


Figure 14. TEM of aggregates of Au nanoparticles functionalized with α -glucopyranosylamide (**13**)

It was observed that the addition of concanavalin-A, a plant lectin which binds specifically to mannose and glucopyranosides, to a solution of the gold nanoparticles and α -glu-OH-S₂ caused significant enhancement in the clustering of gold nanoparticles (Fig. 15).

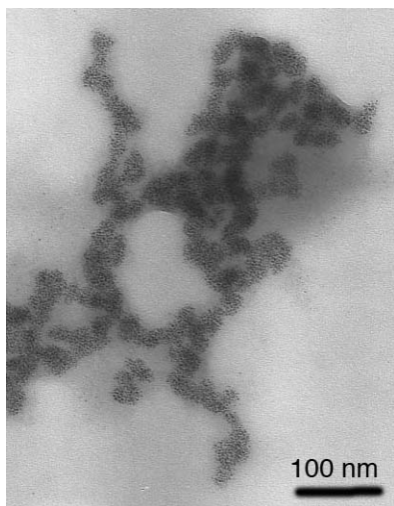


Figure 15. TEM of aggregated Au nanoparticles in the presence of Con A

Some experiments were performed in which the solutions containing α -glu-OH-S₂, gold nanoparticles and Con A were diluted with ethanol in order to observe if the dilution would have any effect on the clustering of the particles. It was observed that there was no effect of dilution on the gold nanoparticle clusters, they stayed intact (Fig. 16).

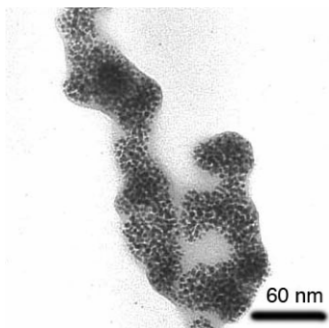


Figure 16. TEM of dilution experiments of Au nanoparticles

UV experiment was also performed on the gold nanoparticles. An absorption around 520 nm indicates a surface plasmon band.⁶²

Conclusion

The synthesis of α - as well as β -linked mono and disaccharides has been studied utilizing the modified Staudinger methodology. This methodology involves the stereoselective synthesis of the glycosylamide linkage utilizing the in situ generated glycosyl isoxazolines. Glycoconjugates have been attached to gold films and formation of both monolayer and multilayered films has been observed depending on the derivative employed. Glycopyranosyl derivatives with free hydroxyl groups gave well ordered, self-assembled monolayers that were characterized by AFM, reflectance FT-IR and XPS analysis. FT-IR and XPS analysis demonstrated that the resulting monolayers were comprised of a hydrogen-bonded network between amides on adjacent sites. Glycoconjugates have also been attached to gold nanoparticles and evidence for aggregation of gold nanoparticles when bound to hydroxylated glycosylamides having thiolated/disulfide side chains has been observed. Also, there is evidence for an enhancement in the aggregation of the gold nanoparticles in the presence of the lectin Concanavalin A which binds specifically to α -linked gluco and mannopyranosides.

Experimental

Thin-layer chromatography (TLC) was performed on 0.25mm Merck silica gel coated plates treated with a UV-active binder with compounds being identified by one or more of the following methods: UV (254 nm) or vanillin. Flash chromatography was performed using thick walled columns and medium pressure silica gel (Whatman 200-425 mesh).

Melting points were taken in Kimax soft glass capillary tubes using a Thomas-Hoover Uni-Melt capillary melting point apparatus (Model 6406 K) equipped with a calibrated thermometer. Melting points above 200°C were taken with a Mel-Temp apparatus using a calibrated thermometer. Melting points are corrected.

Infrared spectra were recorded on a Nicolet 5 DXC FT-IR spectrophotometer. Samples were either dissolved in carbon tetrachloride or prepared as a potassium bromide pellet. Band positions are reported in reciprocal centimeters (cm^{-1}) and relative intensities are listed as br (broad), s (strong), m (medium), or w (weak).

Nuclear magnetic resonance (^1H , ^{13}C NMR) spectra were recorded on a Bruker DRX-400 and Bruker DRX-500 spectrometers. Chemical shifts are reported in parts per million (δ) relative to tetramethylsilane (TMS). Coupling constants (J values) are reported in hertz (Hz), and spin multiplicities are indicated by the following symbols: s (singlet), d (doublet), t (triplet), q (quartet), m (multiplet), br (broad).

Low resolution (LRMS) and high resolution (HRMS) mass spectra were obtained on a VG-7070E magnetic sector instrument.

Tetrahydrofuran (THF) was distilled from sodium/benzophenone ketyl. Methanol (MeOH) was dried and stored over molecular sieves. 1,2-dichloroethane and methylene chloride (CH₂Cl₂) were distilled from calcium hydride and stored over molecular sieves. Triphenylphosphine (Ph₃P) was recrystallized from hexane.

All glassware used in these reactions was dried overnight in an oven at 120°C. All reactions were performed under an atmosphere of argon unless noted otherwise.

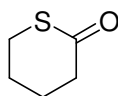
General procedure (A) for the coupling reactions using Ph₃P

The azide (1.0 equiv.) and Ph₃P (1.1 equiv.) were dissolved in anhydrous 1,2-dichloroethane in the presence of 4 Å molecular sieves. The resulting suspension was heated at reflux for 16 h, then cooled to RT. The acylating reagent (1.3 equiv.) and additive (1.3 equiv.) were added to the reaction mixture and the resulting suspension was stirred at the given temperature for 24 h. The reaction mixture was diluted with 100 mL Et₂O and washed with 2 x 100 mL H₂O. The organic layer was dried over Na₂SO₄ and concentrated *in vacuo* to give the crude product, which was purified by flash chromatography.

General procedure (B) for the coupling reactions using Me₃P

The azide (1.0 equiv.) and 1.0 M solution of Me₃P (1.1 equiv.) were dissolved in distilled 1,2-dichloroethane and the resulting solution was stirred for 15 min at RT. The diisopropylethylamine (DIEA) (1.0 equiv.), acylating reagent (1.3 equiv.), and

additive (1.3 equiv.) were added to the reaction mixture and stirred at given temperature for 20 h. The reaction mixture was diluted with 100 mL EtOAc and washed with 2 x 100 mL H₂O. The organic layer was dried over Na₂SO₄ and concentrated *in vacuo* to give the crude product, which was purified by flash chromatography.



Thiolactone (1)

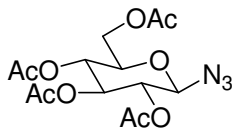
Method I: From 5-Bromovaleric acid

A solution of 5-Bromovaleric acid (0.90 g, 4.9 mmol) was refluxed in 5 mL of thionyl chloride for 2.5 h. The thionyl chloride was then removed under vacuum and the crude acid chloride was dissolved in 5 mL of toluene and slowly added to a solution of sodium hydrogen chalcogenide (NaHS) in 15 mL of H₂O containing tetrabutylammonium hydrogen sulfate (0.30 g). The mixture was stirred at RT for 4 h. The reaction mixture was diluted with Et₂O, washed with 10% aq. Na₂CO₃ solution, dried over Na₂SO₄ and concentrated *in vacuo* to give the crude product which was purified by flash chromatography (hexanes: EtOAc, 7:1) to obtain 98 mg (19%) of the thiolactone as an orange oil.

Method II: From 5-Chlorovaleronitrile

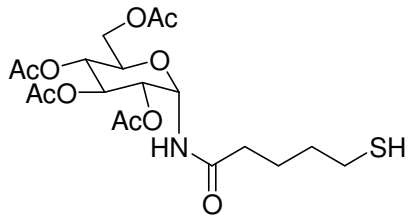
A solution of 5-chlorovaleronitrile (10 g, 0.08 mol) and thiourea (6.5 g, 0.080 mol) in 20 mL of H₂O was refluxed for 2.5 h. A solution of NaOH (17 g, 0.43 mol) dissolved in 50 mL of H₂O was slowly added to the reaction mixture. The reaction mixture turned pink and then colorless. The reaction mixture was refluxed for 36 h open to

air until there was no further evolution of NH_3 as checked by moist pH paper. The reaction mixture was extracted with Et_2O . The aqueous layer was then acidified to pH 4 by adding dil. HCl and then extracted again using EtOAc. Distillation of the oil was carried out under N_2 and 3.59 g (36%) of the thiolactone was obtained as an orange oil, bp = 240-290°C: IR (CCl_4) 3443.6 (s), 2962 (s), 1743 (d), 1451(d), 1249 (s); ^1H NMR (400 MHz, CDCl_3) δ 1.97-2.05 (m, 4H), 2.62 (t, $J = 6.0$, 2H), 3.16 (t, $J = 6.0$, 2H); ^{13}C NMR (100 MHz, CDCl_3) δ 22.8, 23.0, 30.5, 41.3, 201.5.



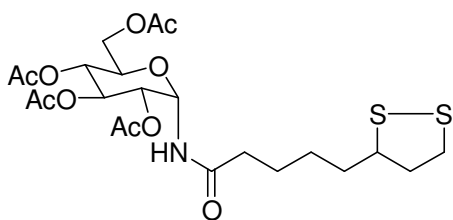
2,3,4,6-Tetra-O-acetyl- β -glucosyl azide (2)

Trimethylsilylazide (2.20 mL, 16.6 mmol) was added to a solution of β -peracetylated glucose (5.0 g, 13 mmol) dissolved in 20 mL of distilled CH_2Cl_2 . 1.0 M SnCl_4 (6.4 mL, 6.4 mmol) was then added and the reaction mixture was stirred for 20 h at 20°C. The reaction mixture was concentrated *in vacuo* and diluted with EtOAc, washed with sat. aq. NaHCO_3 solution and twice with H_2O . The organic layer was dried over Na_2SO_4 and evaporated to give an oil which was recrystallized from absolute ethanol to afford 3.87 g (81%) of the β -azide as a white solid: m.p 123-125°C; IR (neat) 2120 (s), 1752 (s), 1736 (s), 1364 (s), 1236 (s), 1207 (s), 1059 (s), 1037 (s); ^1H NMR (400 MHz, CDCl_3) δ 1.99 (s, 3H), 2.01 (s, 3H), 2.05 (s, 3H), 2.08 (s, 3H), 3.75-3.79 (m, 1H, H5), 4.16 (dd, $J = 12.4$, 2.4, 1H, H6'), 4.24 (dd, $J = 12.4$, 4.8, 1H, H6), 4.63 (d, $J = 8.8$, 1H, H2), 4.94 (t, $J = 9.6$, 1H, H2), 5.08 (t, $J = 9.6$, 1H, H3), 5.20 (t, $J = 9.6$, 1H, H4); ^{13}C NMR (100 MHz, CDCl_3) δ 20.9, 21.1, 21.2, 21.3, 61.8, 62.9, 68.4, 69.0, 69.7, 70.4, 71.9, 72.7, 74.6, 75.5, 87.9, 96.1, 169.8, 169.9, 170.3, 170.5.



2,3,4,6 Tetra-O-acetyl-[5-thiol-1-N-pentanoyl]- α -glucosyl amide (3)

Prepared by the general coupling procedure (A) employing peracetylated glucose- β -azide (0.28 g, 0.77 mmol), Ph_3P (0.22 g, 0.85 mmol) and thiolactone (0.27 g, 2.3 mmol) as the acylating reagent. The reaction mixture was refluxed for 44 h. The residue was purified by flash chromatography (hexanes: EtOAc, 1:1) to give 80 mg (23%) of the glucosyl amide **3** as a yellow oil: IR (CCl_4) 3338 (s), 2958 (s), 2868 (s), 1754 (s), 1705 (s), 1536 (s), 1214 (s); ^1H NMR (400 MHz, CDCl_3) δ 1.74-1.85 (m, 5H), 2.0-2.06 (m, 17H), 2.34 (s, 2H), 3.51 (d, $J = 12.0$, 2H), 3.54 (d, $J = 8.0$, 1H), 4.05-4.13 (m, 2H), 4.26 (dd, $J = 12.0$, 4, 1H), 5.04 (t, $J = 10.0$, 1H), 5.13-5.17 (m, 1H), 5.34 (t, $J = 10.0$, 1H), 5.87 (t, $J = 8.0$, 1H), 6.83 (d, $J = 8.0$, 1H, NH).



2,3,4,6-Tetra-O-acetyl-[3-(1,2-Dithiacyclopentyl)]-1-N-pentanoyl- α -glucosyl amide (4)

From 2-fluoro-1-methyl-pyridinium p-toluene sulfonate

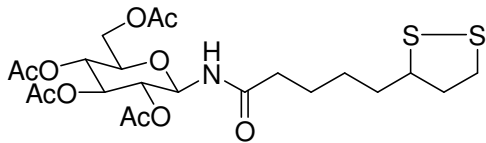
A solution of glucose- β -azide (0.25 g, 0.67 mmol), Ph_3P (0.19 g, 0.74 mmol) and molecular sieves were refluxed in 6 mL of 1,2-dichloroethane for 16 h. The reaction mixture was cooled to RT. A solution of FMPPTS (0.26 g, 0.91 mmol) was dissolved in CH_2Cl_2 and cooled to -10°C . Another flask was charged with thioctic acid (0.18 mg, 0.87 mmol) in 6-8 mL of CH_2Cl_2 and Et_3N (121 μL) was added dropwise into the solution. The acid- Et_3N solution was transferred into the FMPPTS solution via cannula and the resulting solution was stirred at -10°C for 1 h. The sugar solution was added into this solution via cannula and stirred at RT for 24 h. The reaction mixture was diluted with 100 mL EtOAc and washed with 100 mL H_2O . The organic layer was dried over Na_2SO_4 and concentrated *in vacuo* to give the crude product, which was purified by flash chromatography (hexanes: EtOAc 1:1) to give 55 mg (15%) of the glucosyl amide **4** as an α/β mixture.

From thioctoyl chloride

Prepared by the general coupling procedure (A) employing peracetylated glucose- β -azide (0.25 g, 0.67 mmol), Ph_3P (0.19 g, 0.74 mmol) and thioctic acid chloride (0.23 g, 1.0 mmol) as the acylating agent. The reaction mixture was refluxed for 24 h. The residue was purified by flash chromatography (hexanes: EtOAc, 1:1) to give 88 mg (25%) of the glucosyl amide **4**.

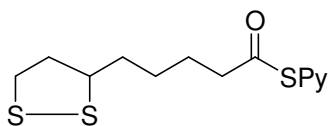
From thioctic ester

Prepared by the general coupling procedure (A) employing peracetylated glucose- β -azide (1.0 g, 2.7 mmol), Ph_3P (0.77 g, 2.9 mmol), thioctic ester (1.1g, 3.5 mmol) as the acylating reagent and $\text{CuCl}_2 \cdot 2\text{H}_2\text{O}$ (0.59 g, 3.5 mmol) as the additive respectively. The reaction mixture was stirred at RT for 24 h. The residue was purified by flash chromatography (hexanes: EtOAc, 1: 2) to give 784 mg (55%) of the glucosyl amide **4**: IR (CCl_4) 3300 (s), 2930 (s), 2854 (s), 1757 (s), 1702 (s), 1217 (s); ^1H NMR (400 MHz, CDCl_3) δ 1.42-1.54 (m, 2H), 1.61-1.70 (m, 4H), 1.85-1.93 (m, 1H), 2.01 (s, 9H), 2.06 (s, 3H), 2.29 (t, $J = 6.8$, 2H), 2.34-2.50 (m, 1H), 3.12 (m, 2H), 3.54 (p, $J = 8.0, 6.4$, 1H), 3.89 (m, 1H), 4.05 (dd, $J = 12.0, 10.4$, 1H), 4.25 (dd, $J = 12.4, 4.4$, 1H), 5.03 (t, $J = 9.6$, 1H), 5.16 (m, 1H), 5.28 (t, $J = 10.0$, 1H), 5.83 (m, 1H), 6.1 (d, $J = 5.2$, 1H, NH); ^{13}C NMR (100 MHz, CDCl_3) δ 14.6, 20.9, 21.0, 21.0, 21.1, 25.5, 29.2, 34.9, 36.6, 38.8, 40.6, 56.7, 62.1, 68.4, 68.7, 70.5, 74.6, 169.3, 169.8, 170.8, 171.1, 173.6; LRMS (FAB) 536 ($\text{M} + \text{H}$) $^+$, 542 ($\text{M} + \text{Li}$) $^+$.



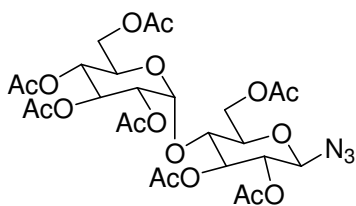
2,3,4,6-Tetra-O-acetyl-[3-(1,2-Dithiacyclopentyl)]-1-N-pentanoyl- β -glucosyl Amide (5)

Prepared by the general coupling procedure (B) employing peracetylated glucose- β -azide (0.25 g, 0.67 mmol), a 1.0 M solution of Me₃P (0.87 mL, 0.87 mmol), DIEA (0.12 mL, 0.67 mmol) and thioctic ester (0.40 g, 1.3 mmol) as the acylating agent. The reaction mixture was stirred at RT for 20 h. Purification of the residue by flash chromatography (hexanes: EtOAc, 1:2) gave 253 mg (70%) of the glucosyl amide **5** as an oil; IR (CCl₄) 3430 (s), 2937 (s), 2859 (s), 1761 (s), 1705 (s), 1507 (s), 1228 (s); ¹H NMR (400 MHz, CDCl₃) δ 1.20-1.40 (m, 2H), 1.51-1.63 (m, 4H), 1.73-1.82 (m, 1H), 1.89 (s, 3H), 1.91 (s, 3H), 1.93 (s, 3H), 1.96 (s, 3H), 2.02-2.15 (m, 2H), 2.30-2.40 (m, 1H), 2.96-3.08 (m, 2H), 3.44 (m, 1H), 3.74 (br d, J = 10.0, 1H, H5), 3.94-4.0 (m, 1H), 4.20 (dd, J = 12.4, 4.0, 1H, H6), 4.80 (t, J = 9.6, 1H), 4.93 (t, J = 9.6, 1H), 5.2 (m, 2H), 6.45 (d, J = 9.2, 1H, NH); ¹³C NMR (100 MHz, CDCl₃) δ 20.5, 20.6, 20.7, 24.7, 25.2, 25.5, 26.4, 28.6, 28.7, 28.8, 29.5, 31.5, 33.1, 34.5, 36.1, 36.2, 36.6, 38.4, 40.2, 56.2, 56.4, 61.6, 68.1, 70.6, 72.7, 73.4, 169.5, 169.8, 170.5, 170.8, 170.9, 171.1, 173.0; LRMS (nba-peg) 535 (M)⁺, 536 (M + H)⁺. There are eleven carbons (33) more than expected (22), due to the diastereotopic nature of the molecule.



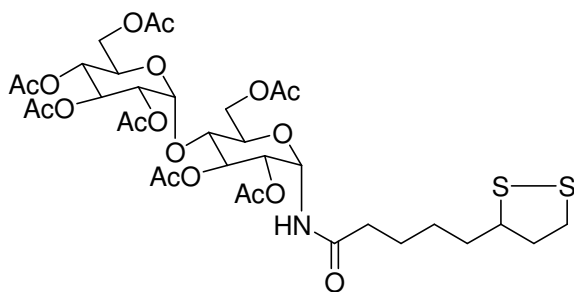
Thioctic ester (6)

A solution of thioctic acid (1.0 g, 4.9 mmol), Ph_3P (1.6 g, 6.2 mmol) and dithiodipyridine (1.4 g, 6.2 mmol) in 15 mL of THF was stirred at RT for 24 h. The THF was evaporated and flash chromatography of the residue (hexanes: EtOAc, 2:1) gave 1.4 g (96%) of the thiopyridyl ester as an oil: IR (CCl_4) 3048 (s), 2959 (s), 2924 (s), 2855 (s), 1741 (s), 1708 (s), 1544 (w), 1374 (s); ^1H NMR (400 MHz, CDCl_3) δ 1.43-1.53 (m, 2H), 1.65-1.77 (m, 4H), 1.86-1.91(m, 1H), 2.40-2.48 (m, 1H), 2.70 (t, $J = 7.4$, 2H), 3.06-3.19 (m, 2H), 3.51-3.58 (m, 1H), 7.23 (ddd, $J = 0.8$, 4.8, 1H), 7.59 (d, $J = 6.0$, 1H), 7.66-7.76 (m, 1H), 8.6 (dd, $J = 4.8$, 0.8, 1H), ^{13}C NMR (100 MHz, CDCl_3) δ 25.4, 28.9, 34.9, 38.9, 40.6, 44.3, 56.6, 124.1, 130.7, 138.0, 150.9, 196.3; LRMS (FAB) 300 ($\text{M} + \text{H}$) $^+$.



2, 3, 6- Tri-O-acetyl-4-O-[2,3,4,6 –tetra-O-acetyl- α -D-glucopyranosyl]- β -D-glucopyranosyl azide (hepta-O-acetyl- β -maltosyl azide) (7)

Trimethylsilylazide (0.63 mL, 4.7 mmol) was added via syringe followed by 1.0 M SnCl₄ (3.39 mL, 3.39 mmol) to octa-O-acetyl- β -maltose (2.3 g, 3.4 mmol) dissolved in 25 mL of distilled CH₂Cl₂ and the reaction mixture was stirred for 20 h at RT. The crude reaction mixture was concentrated *in vacuo* and diluted with EtOAc, washed with sat. aq. NaHCO₃ solution and twice with H₂O. The organic layer was dried over Na₂SO₄ and evaporated to give an oil which was recrystallized from absolute ethanol to afford 1.93 g (86%) of β -azide **7** as a white solid: m.p 114-116°C ; IR (CCl₄) 2958 (w), 2122 (s), 1761 (s), 1368 (s), 1228 (s); ¹H NMR (400 MHz, CDCl₃) δ 2.03 (s, 3H), 2.04 (s, 3H), 2.05 (s, 3H), 2.07 (s, 3H), 2.08 (s, 3H), 2.13 (s, 3H), 2.18 (s, 3H), 3.80-3.82 (m, 1H), 3.96-3.99 (m, 1H), 4.02-4.09 (m, 1H), 4.14 (d, *J* = 7.2, 1H), 4.25-4.30 (m, 3H), 4.52 (dd, *J* = 12.4, 2.4, 1H), 4.72 (d, *J* = 8.8, 1H), 4.81 (t, *J* = 8.8, 1H), 4.88 (dd, *J* = 10.8, 4.0, 1H), 5.08 (t, *J* = 10.0, 1H), 5.26-5.33 (m, 1H), 5.35-5.41 (m, 1H), 5.43 (d, *J* = 4.0, 1H); ¹³C NMR (100 MHz, CDCl₃) δ 20.9, 21.1, 21.2, 21.3, 21.4, 61.8, 62.9, 68.3, 69.0, 69.7, 70.1, 70.4, 71.9, 72.7, 72.8, 74.7, 75.5, 87.9, 96.1, 169.8, 169.9, 170.3, 170.5, 170.8, 170.9, 170.9; LRMS (FAB) 668 (M + Li)⁺.

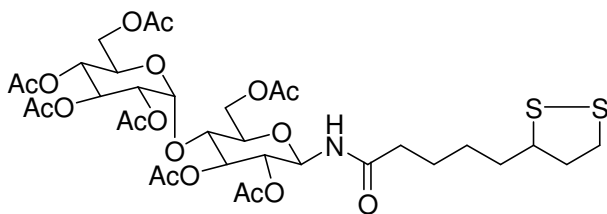


Heptaacetate-[3-(1,2- Dithiacyclopentyl)]-1-

N-pentanoyl- α -maltosyl amide (**8**)

Prepared by the general coupling procedure (A) employing hepta-O-acetyl- β -D-maltose azide (1.0 g, 1.5 mmol), Ph_3P (0.43 g, 1.6 mmol), thioctic ester (0.62 g, 1.9 mmol) as the acylating reagent, and $\text{CuCl}_2 \cdot 2\text{H}_2\text{O}$ (0.33 g, 1.9 mmol) as the additive. The reaction mixture was stirred at RT for 24 h. The residue was purified by flash chromatography (hexanes: EtOAc, 1: 3) to give 0.98 g (79%) of the maltosyl amide **8** as a gummy oil: IR (CCl_4) 3373 (s), 2983 (s), 2937 (s), 1744 (s), 1704 (s), 1373 (s); ^1H NMR (400 MHz, CDCl_3) δ 1.42-1.56 (m, 2H), 1.62-1.74 (m, 4H), 1.86-1.96 (m, 1H), 2.01 (s, 9H), 2.06 (s, 3H), 2.29 (s, 6H), 2.08 (s, 3H), 2.10 (s, 3H), 2.14 (s, 3H), 2.20 (s, 3H), 2.31-2.36 (m, 1H), 3.10-3.19 (m, 1H), 3.96 (m, 1H), 3.96-4.07 (m, 2H), 4.08-4.14 (m, 2H), 4.21-4.27 (m, 3H), 4.44 (dd, $J = 12.4, 2.4$, 1H), 4.87 (dd, $J = 10.0, 4.0$, 1H), 4.95 (dd, $J = 10.0, 3.6$, 1H), 5.08 (t, $J = 10.0$, 1H), 5.39 (t, $J = 10.0$, 1H), 5.43 (d, $J = 4.0$, 1H), 5.49 (t, $J = 8.8$, 1H), 6.25 (d, $J = 3.6$, 1H, NH); ^{13}C NMR (100 MHz, CDCl_3) δ 14.5, 20.8, 20.8, 20.9, 20.9, 21.0, 21.1, 21.2, 21.3, 25.3, 29.0, 34.9, 38.7, 40.5, 56.6, 60.7, 61.8, 63.1, 68.3, 68.7, 69.1, 69.5, 70.4, 72.2, 73.5, 96.4, 120.0, 121.5, 128.8, 128.9, 169.6, 169.7, 170.2, 170.3, 170.6, 170.7, 170.8, 170.9, 171.6,

173.8. LRMS (FAB) 823 (M)⁺, 824 (M + H)⁺, 956 (M + Cs)⁺. There are six carbons (40) more than expected (34), due to the diastereotopic nature of the molecule.



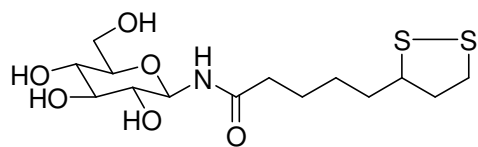
Heptaacetate-[3-(1,2-Dithiacyclopentyl)]-1-N-pentanoyl- β -maltosyl amide (9)

Prepared by the general coupling procedure (B) employing hepta-O-acetyl- β -D-maltose azide (0.25 g, 0.38 mmol), a 1.0 M solution of Me₃P (0.491 mL, 0.491 mmol), DIEA (65.7 μ L, 0.380 mmol) and thioctic ester (0.23 g, 0.76 mmol) as the acylating agent. Purification of the residue by flash chromatography (hexanes: EtOAc, 1: 3) gave 130 mg (42%) of the maltosyl amide **9** as an oil: IR (neat) 2926 (s), 1741 (s), 1665 (s), 1534 (s), 1366 (s), 1214 (s); ¹H NMR (400 MHz, CDCl₃) δ 1.40 - 1.45 (m, 2H), 1.58-1.69 (m, 4H), 1.83-1.91 (m, 1H), 1.98 (s, 6H), 2.00 (s, 6H), 2.04 (s, 3H), 2.07 (s, 3H), 2.11 (s, 3H), 2.14-2.21 (m, 2H), 2.39-2.47 (m, 1H), 3.05-3.18 (m, 2H), 3.51 (p, *J* = 12.4, 1H), 3.76 (br d, *J* = 7.6, 1H, H5), 3.94 (m, 2H), 4.04 (br d, *J* = 12.4, 1H), 4.19 (m, 2H, H6, H6'), 4.39 (br d, *J* = 12.4, 1H, H6), 4.72 (t, *J* = 9.6, 1H, H2), 4.83 (dd, *J* = 10.4, 4.0, 1H, H2'), 5.01 (t, *J* = 9.6, 1H, H4'), 5.25 (t, *J* = 9.6, 1H, H1), 5.33 (t, *J* = 9.6, 1H, H3'), 5.37 (d, *J* = 2.4, 1H, H1'), 6.00 (d, *J* = 8.8, 1H, NH); ¹³C NMR (100 MHz, CDCl₃) δ 20.9, 21.0, 21.0, 21.2, 25.1, 25.1, 29.0, 29.8, 30.0, 34.9, 34.9, 36.6, 36.7, 38.8, 40.6, 40.7, 56.6, 60.7, 61.8, 63.1, 68.3, 68.9, 69.6,

70.3, 71.7, 73.0, 74.3, 75.3, 95.9, 169.8, 170.0, 170.2, 170.8, 170.9, 170.0, 171.5, 171.5, 173.2, 173.2; LRMS (FAB) 830 ((M + Li)⁺, 100); 824(M + H)⁺. There are five carbons (39) more than expected (34) due to the diastereotopic nature of the molecule.

General Hydroxylation procedure

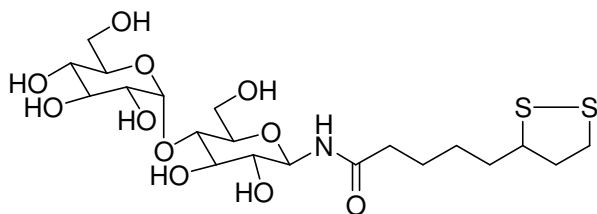
Sodium (0.25 g) was added to 50 mL of MeOH solution and after all the sodium had reacted the sugar solution was dissolved in 5-6 mL MeOH in a separate flask and the NaOMe solution was added to it via syringe and stirred at RT for 20 h. Amberlite IR-120 (H⁺) acidic resin was added until the solution turns slightly acidic or neutral. The residue was filtered and concentrated *in vacuo* to give the product.



[3-(1,2-Dithiacyclopentyl)]-1-N-pentanoyl- β -glucosyl amide (11)

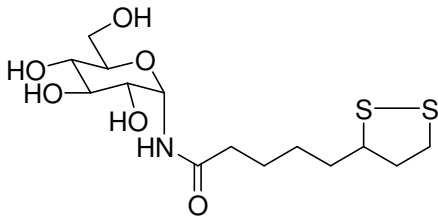
Prepared by the general procedure for hydroxylation employing peracetylated glucosyl disulfide (0.15 g, 0.28 mmol) in 5-6 mL of MeOH. The NaOMe solution (5-6 mL) was transferred to the sugar solution and stirred at RT for 20 h. The reaction mixture was concentrated *in vacuo* to yield 70 mg (68%) of the glucosylamide **11** as a red oil: IR (neat) 3403 (s), 2974 (s), 2479 (s), 1454 (s), 1055 (s); ¹H NMR (400 MHz, CDCl₃) δ 1.34-1.35 (m, 2H), 1.53-1.55 (m, 4H), 1.62-1.65 (m, 1H), 1.86-1.90 (m, 1H), 2.14-2.25 (m, 1H), 2.36-2.40 (m, 1H), 3.09-3.12 (m, 1H), 3.26- 3.80 (m, 7H),

4.85 (d, $J = 8.8$, 1H, NH); ^{13}C NMR (100 MHz, CDCl_3) δ 17.1, 25.1, 28.2, 34.1, 35.8, 38.4, 40.6, 56.8, 57.8, 60.9, 69.6, 72.1, 76.9, 79.6, 178.6; LRMS (FAB, negative ion) 366 (M-1) $^{-1}$.



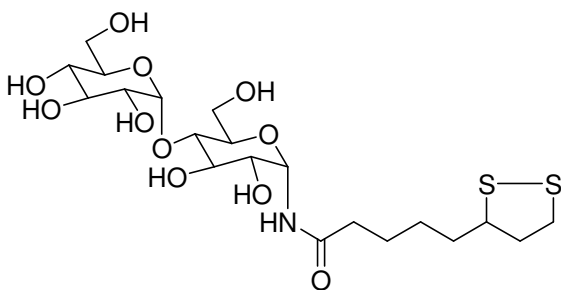
[3-(1,2-Dithiacyclopentyl)]-1-N-pentanoyl- β -maltosyl amide (12)

Prepared following the general procedure for hydroxylation employing β -maltosyl azide (0.05 g, 0.06 mmol) dissolved in 3-5 mL of MeOH. The NaOMe solution (5 mL) was transferred into the sugar solution and stirred at RT for 20 h. Amberlite IR-120 (H^+) resin was added until the solution turned slightly acidic or neutral. The reaction mixture was filtered and concentrated *in vacuo* to yield 24 mg (30 %) of the maltosyl amide **12** as an orange oil: IR (neat) 3416 (w), 2926 (s), 2493 (w), 1707 (s); ^1H NMR (400 MHz, CDCl_3) δ 1.24-1.27 (m, 2H), 1.45-1.55 (m, 4H), 1.77-1.82 (m, 1H), 2.14-2.17 (m, 2H), 2.99-3.0 (m, 1H), 3.24-3.29 (t, $J = 8.8$, 2H), 3.41-3.75 (m, 7H), 4.74 (d, $J = 8.8$, 1H); ^{13}C NMR (100 MHz, CDCl_3) δ 23.5, 25.1, 25.2, 25.7, 28.7, 29.1, 33.9, 34.1, 34.7, 35.0, 36.4, 38.8, 38.9, 39.0, 40.7, 56.8, 56.9, 60.8, 61.0, 69.6, 71.9, 72.1, 73.0, 73.2, 76.5, 77.0, 77.3, 79.5, 100.13, 177.9, 181.5; LRMS (FAB, negative ion) 528 (M-1) $^{-1}$.



**[3-(1,2-Dithiacyclopentyl)]-1-N-pentanoyl- α -
glucosyl amide (13)**

Prepared by the general procedure for hydroxylation employing peracetylated glucosyl sugar (0.50 g, 0.93 mmol) in 5 mL of anhydrous MeOH. The NaOMe solution (6-8 mL) was transferred into the sugar solution via syringe and stirred for 20 h. The solution was filtered and the MeOH was concentrated *in vacuo* to give 256 mg (57%) of the glucosyl amide **13**: IR (neat) 3325 (w), 2925, 1714, 1666 (s), 1535 (s), 1371(s). ^1H NMR (400 MHz, CDCl_3) δ 1.27- 1.32 (m, 2H), 1.47-1.62 (m, 4H), 1.83-1.87 (m, 1H), 2.20-2.27 (m, 2H), 2.32-2.37 (m, 1H), 3.04-3.10 (m, 2H), 3.29-3.36 (m, 2H), 3.51-3.70 (m, 6H), 5.44 (d, $J = 5.6$, 1H, NH) ; ^{13}C NMR (100 MHz, CDCl_3) δ 22.7, 25.4, 28.2, 28.3, 34.1, 34.2, 35.6, 35.7, 38.5, 40.6, 40.6, 56.8, 56.9, 60.8, 69.7, 73.0, 73.3, 76.9, 179.0, 180.2; LRMS (FAB, negative ion) 366 (M-1) $^{-1}$.



[3-(1,2-Dithiacyclopentyl)]-1-N-pentanoyl- α -maltosyl amide (14)

Prepared following the general procedure for hydroxylation employing maltose octaacetate (1.2 g, 0.0014 mol) in 6-8 mL of MeOH. The NaOMe solution (8 mL) was transferred into the sugar solution and stirred at RT for 20 h. The reaction mixture was filtered and concentrated *in vacuo* to yield 299 mg (40 %) of the maltosyl amide **14** as an orange oil: IR (neat) 3304(w), 2925(s), 1656(s), 1529(s), 1034(s); ^1H NMR (400 MHz, CDCl_3) δ 1.31-1.37 (m, 2H), 1.50-1.70 (m, 4H), 1.85-2.01 (m, 1H), 2.21-2.37 (m, 2H), 2.38-2.43 (m, 1H), 3.09-3.16 (m, 2H), 3.34 (t, $J = 9.6$, 1H), 3.48-3.77 (m, 11H), 3.88 (m, 1H), 5.31 (m, 1H), 5.48 (d, $J = 5.6$, 1H, NH); ^{13}C NMR (100 MHz, CDCl_3) δ 17.1, 25.3, 28.0, 34.0, 35.7, 38.4, 40.6, 56.9, 60.8, 69.5, 71.6, 72.1, 73.1, 73.8, 76.7, 100.1, 129.4, 132.3, 179.3; LRMS (FAB, negative ion) 528 ($\text{M}-1$) $^{-1}$.

Preparation of gold films

Gold films on single-crystal Si (001) wafers were used as substrates. Prior to the deposition of the films, the wafers were washed using a “piranha solution” consisting of 70 % H_2SO_4 and 30 % H_2O_2 . After washing, a Cr adhesion layer (20 nm) was

deposited by vapor deposition, followed by 200 nm of Au. Each substrate was again cleaned with piranha solution and rinsed thoroughly with deionized water (18.3 MΩ) immediately prior to immobilizing the sugars.

Deposition of the sugars on gold films

A 1 mM solution of the sugars was prepared and the gold films were soaked in about 2-3 mL of the sugar solution for around 2 h. The gold film was taken out of solution, rinsed with deionized water and dried with N₂.

FT-IR measurements of gold films

FT-IR absorption spectra were measured in a Digilab FTS7000 series spectrometer with a PIKE Technologies wire grid infrared polarizer (p polarized) and a Vee Max variable angle specular reflectance accessory (reflectance angle 75°). Spectra (1800-1300 cm⁻¹) were collected from 2000 scans at 2 cm⁻¹ resolution using a cryogenic mercury cadmium telluride detector.

XPS studies of gold films

The X-ray photoelectron measurements were performed using a Kratos Axis 165 spectrometer at a vacuum of 4×10^{-10} Torr with monochromatic AlK α radiation. The X-ray power used for the measurements was 144 W. The samples were introduced into the vacuum chamber using a conductive carbon tape. A wide scan survey and various slots of regions (Au 4f, S 2p, N 1s, O 1s and C 1s) were measured. All measurements were performed in hybrid mode using both electrostatic and magnetic

lenses, with a step size of 0.1 eV and sweep time of 60 s. All individual region spectra were recorded in the FAT analyzer mode with pass energy of 80 eV, and an average of 10 scans. The energy resolution during acquisition of single region-scan was about 1.0 eV. Charge neutralizer was off during the measurements and binding energy calibration was done with respect to Au 4f at 84.0 eV.

Analysis of the data

Data processing was performed using Vision processing software. After subtraction of a linear background, spectra were fitted using 60% Gaussian / 40% Lorentzian peaks, taking the minimum number of peaks consistent with the best fit. The important parameters used for this fitting were peak position, full width at half maximum, intensity and the Gaussian fraction which determines the fraction of the Gaussian component in the fitted peak shape.

Contact Angle Measurements

Contact Angles were measured on horizontal profiles of sessile drops of water (4-5 μL) using a 5X eye piece. Images were taken using a Pelco black and white video camera.

Synthesis of Gold nanoparticles

The gold nanoparticles were synthesized according to the procedure by Hutchison.⁶³ Hydrogen tetrachloroaurate trihydrate and tetraoctylammonium bromide were dissolved in a nitrogen sparged water/ toluene mixture (50 mL/ 65 mL). When the

golden color had transferred the organic phase turned white and cloudy. Aqueous NaBH_4 dissolved in H_2O (10 mL) was rapidly added. The organic phase immediately turned dark purple after which it was stirred for 3h under nitrogen. The toluene layer was separated and washed with H_2O (2 x 100 mL). The solvent was removed with a stream of nitrogen to yield a black solid. The residue was subjected to the following series of washes: (200 mL hexanes, 100 mL of H_2O), 5 x (100 mL hexanes followed by 100 mL of methanol: H_2O (2:3), 5 x (100 mL of hexanes followed by 100 mL of saturated aq. NaNO_2), 5 x (100 mL of hexanes followed by MeOH: H_2O (2:3), 5 x (100 mL of hexanes followed by 100 mL of aq. NaNO_2), 5 x (100 mL of hexanes followed by MeOH: H_2O (2:3). Further purification was accomplished by precipitation from CHCl_3 by slow addition of pentane to yield 295 mg of gold nanoparticles. TEM analysis indicated that the size distribution was 3-5 nm.

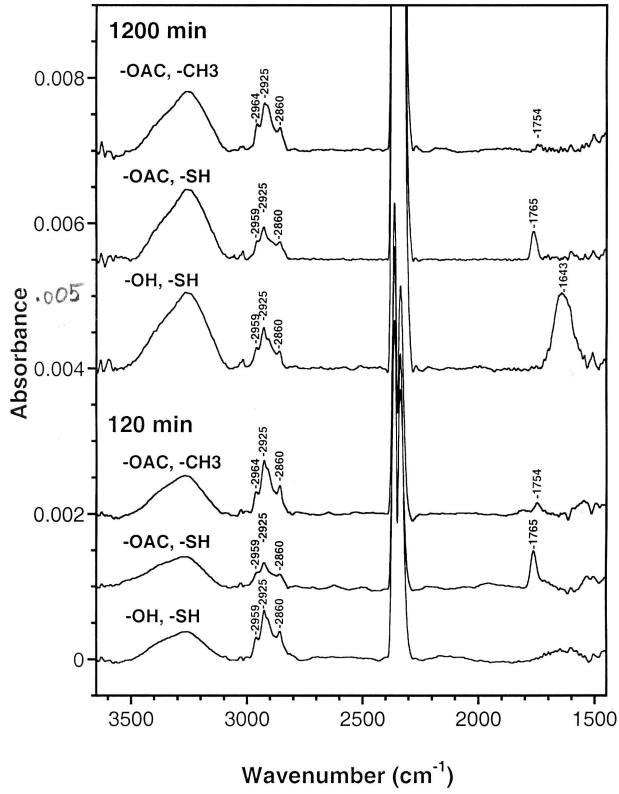
For all TEM experiments measured 2-4 μL of the glucosylamide solutions on a copper grid with formvar coating.

- 1) Prepared a solution of Au nanoparticles (6 mg, 0.03 mmol) in 25 mL of CH_2Cl_2 .
- 2) Prepared a solution of Au nanoparticles (3 mg, 0.015 mmol) and α -glu-OH-SH (2 mg, 0.006 mmol) dissolved in 50 mL of CH_2Cl_2 for an hour.
- 3) Prepared a 12 mM solution of α -glu-OH-S₂ in EtOH. Au nanoparticles (3 mg, 0.015 mmol) dissolved in EtOH were soaked in 0.68 mL of the sugar solution for an hour. Diluted with EtOH upto 10 mL in a graduated flask.

4) Au nanoparticles (3 mg, 0.015 mmol) dissolved in EtOH were added to 2.7 mL of a 12 mM solution of α -glu-OH-S₂. The solution was diluted with EtOH till it reached the right concentration for TEM.

5) Au nanoparticles (5 mg, 0.03 mmol) dissolved in EtOH were added to 3.5 mL of a 14 mM solution of α -glu-OH-S₂. 3 mL of Con-A solution prepared in a buffer of 0.15 M NaCl and 0.025 M Na₂HPO₄ was added to the sugar solution and the solution was diluted with H₃PO₄ till the pH of the solution turned 5.0.

Appendix: Raw data for FT-IR of thiolated oligosaccharides



References

- ¹ Miller, D. J. Macek,; Schur, B. D. *Nature* **1992**, 258, 964-969.
- ² (a) Varki, A. *Glycobiology* **1993**, 3, 97-130. (b) Dwek, R. A. *Chem. Rev.* **1996**, 96, 683-720. (c) Kobata, A. *Glycoconjugate J.* **2000**, 17, 443-464. (c) Herzner, H.; Reipen, T.; Schultz, M.; Kunz, H. *Chem. Rev.* **2000**, 100, 4495-4537.
- ³ Anisfeld, S. T.; Lansbury, P. T. *J. Am. Chem. Soc.* **1993**, 115, 10531-10537.
- ⁴ Anisfeld, S. T.; Lansbury, P. T. *J. Org. Chem.* **1990**, 55, 5560-5562.
- ⁵ Arsequell, G.; Valencia, G. *Tetrahedron: Asymmetry* **1999**, 10, 3045-3094.
- ⁶ Likhoshesterov, L. M.; Novikova, O. S.; Dervitskaja, V. A.; Kochetkov, N. K. *Carbohydr. Res.* **1986**, 46, C1.
- ⁷ Lubineau, A.; Auge, J.; Drouillat, B. *Carbohydr. Res.* **1995**, 266, 211-219.
- ⁸ Teshima, T.; Nakajima, K.; Takahashi, M.; Shiba, T. *Tetrahedron Lett.* **1992**, 33, 363-366.
- ⁹ Thiem, J.; Wiemann, T. *Angew. Chem., Int. Ed. Engl.* **1990**, 29, 80-82.
- ¹⁰ Mehta, S.; Meldal, S.; Duus, J. O.; Bock, K. *J. Chem. Soc., Perkin Trans. 1* **1999**, 1445-1451.
- ¹¹ Marks, G. S.; Marshall, R. D.; Neuberger, A. *Biochem. J.* **1963**, 87, 274-281.
- ¹² McDonald, F. E.; Danishefsky, S. J. *J. Org. Chem.* **1992**, 57, 7001-7002.
- ¹³ Unverzagt, C. *Angew. Chem., Int. Ed. Engl.* **1996**, 35, 2350-2353.
- ¹⁴ Garcia-Lopez, J. J.; Santoyo-Gonzalez, F.; Vargas-Berenguel, A. *Synlett* **1997**, 265-266.
- ¹⁵ Matsuo, T.; Nakahara, Y.; Ito, Y.; Nukada, T.; Ogawa, T. *Bioorg. Med. Chem.* **1995**, 3, 1455-1463.
- ¹⁶ Gyorgydeak, Z.; Szilagy, L.; Paulsen, H. *J. Carbohydr. Chem.* **1993**, 12, 139-163.
- ¹⁷ Soli, E. D.; DeShong, P. *J. Org. Chem.* **1999**, 64, 9724-9726.

- ¹⁸ Soli, E. D.; Manoso, A. S.; Patterson, M. C.; DeShong, P.; Favor, D. A.; Hirschmann, R.; Smith, A. B. *J. Org. Chem.* **1999**, *64*, 3171-3177.
- ¹⁹ Garcia-Lopez, J. J.; Santoyo-Gonzalez, F.; Vargas-Berenguel, A. *Synlett* **1997**, 265-266.
- ²⁰ Gololobov, Y. G.; Kasukhin, L. F. *Tetrahedron* **1992**, *48*, 1353-1406.
- ²¹ Gololobov, Y. G.; Zhmurova, I. N.; Kasukhin, L. F. *Tetrahedron* **1981**, *37*, 437-472.
- ²² Gyorgydeak, Z.; Szilagy, L.; Paulsen, H. *J. Carbohydr. Chem.* **1993**, *12*, 139.
- ²³ Garcia, J.; Urpi, F.; Vilarrasa, J. *Tet. Lett.* **1984**, *25*, 4841-4844.
- ²⁴ Inazu, T.; Kobayashi, K. *Synlett* **1993**, 869-870.
- ²⁵ Maunier, V.; Boullanger, P.; Lafont, D. *J. Carbohydr. Chem.* **1997**, *16*, 231-235.
- ²⁶ Isac-Garcia, J.; Calvo-Flores, F. G.; Hernandez-Mateo, F.; Santoyo-Gonzalez, F. *Eur. J. Org. Chem.* **2001**, 383-390.
- ²⁷ Ratcliffe, A. J.; Fraser-Reid, B. *J. Chem. Soc., Perkin Trans. 1* **1990**, 747-751.
- ²⁸ Damkaci, F.; DeShong, P. *J. Am. Chem. Soc.* **2003**, *125*, 4408-4409.
- ²⁹ Fuente, J. M.; Barrientos, A. G.; Rojas, T. C.; Rojo, J.; Canada, J.; Fernandez, A.; Penades, S. *Angew. Chem., Int. Ed.* **2001**, *40*, 2258-2261.
- ³⁰ Otsuka, H.; Akiyama, Y.; Nagasaki, Y.; Kataoka, K. *J. Am. Chem. Soc.* **2001**, *123*, 8226-8230.
- ³¹ Rojas, T. C.; Fuente, J. M. *Adv. Mater.* **2002**, *14*, 585-588.
- ³² Barrientos, A. G.; Fuente, J. M.; Rojas, T. C.; Fernandez, A.; Penadés, S. *Chem. Eur. J.* **2003**, *9*, 1909-1921.
- ³³ Rojo, J.; Diaz, V.; Fuente, J.; Segura, I.; Barrientos, A. G.; Riese, H. H.; Bernad, A.; Penadés, S. *Chem Bio Chem* **2004**, *5*, 291-297.
- ³⁴ Lin, C. C.; Yeh, Y. C.; Yang, C.; Chen, C. L.; Chen, G. F.; Chen, C. C.; Wu, Y. C. *J. Am. Chem. Soc.* **2002**, *124*, 3508-3509.

- ³⁵ Lin, C. C.; Yeh, Y. C.; Yang, C. Y.; Chen, G. F.; Chen, Y. C.; Wu, Y. C.; Chen, C. C. *J. Chem. Soc., Chem. Commun.* **2003**, 2920-2921.
- ³⁶ Lis, H.; Sharon, N. *Chem. Rev.* **1998**, *98*, 637.
- ³⁷ Shenhar, R.; Rotello, V. M. *Acc. Chem. Res.* **2003**, *36*, 549-561.
- ³⁸ Ulman, A. *Chem. Rev.* **1996**, *96*, 1533-1554.
- ³⁹ (a) Porter, M. D.; Bright, T. B.; Allara, D. L.; Chidsey, C. E. D. *J. Am. Chem. Soc.* **1987**, *109*, 3559-3568. (b) Troughton, E. B.; Bain, C. D.; Whitesides, G. M.; Nuzzo, R. G.; Allara, D. L.; Porter, M. D. *Langmuir* **1988**, *4*, 365-385. (c) Bain, C. D.; Troughton, E. B.; Tao, Y.-I.; Evall, J.; Whitesides, G. M.; Nuzzo, R. G. *J. Am. Chem. Soc.* **1989**, *111*, 321-335. (d) Laibinis, P. E.; Whitesides, G. M.; Allara, D. L.; Tao, Y.-T.; Parikh, A. N.; Nuzzo, R. G. *J. Am. Chem. Soc.* **1991**, *113*, 7152-7167. (e) Bryant, M. A.; Joa, S. L.; Pemberton, J. E. *Langmuir* **1992**, *8*, 753.
- ⁴⁰ Bain, C. D.; Whitesides, G. M. *Adv. Mater.* **1989**, *1*, 506.
- ⁴¹ Lee, T. R.; Laibinis, P. E.; Folkers, J. P.; Whitesides, G. M. *Pure Appl. Chem.* **1991**, *63*, 821.
- ⁴² Whitesides, G. M.; Ferguson, G. S. *Chemtracts-Org. Chem.* **1988**, *1*, 171.
- ⁴³ Sellers, H.; Ulman, A.; Shnidman, Y.; Eilers, J. E. *J. Am. Chem. Soc.* **1993**, *115*, 9389.
- ⁴⁴ Ulman, A. *J. Mater. Educ.* **1989**, *11*, 205.
- ⁴⁵ Bain, C. D.; Whitesides, G. M. *Science* **1988**, *1*, 171.
- ⁴⁶ Bain, C. D.; Whitesides, G. M. *J. Am. Chem. Soc.* **1988**, *110*, 6560.
- ⁴⁷ Bain, C. D.; Whitesides, G. M. *J. Am. Chem. Soc.* **1988**, *110*, 5897.
- ⁴⁸ Nuzzo, R. G.; Dubois, L. H.; Allara, D. L. *J. Am. Chem. Soc.* **1990**, *112*, 558.
- ⁴⁹ Boal, A. K.; Rotello, V. M. *Langmuir* **2000**, *16*, 9527-9532.
- ⁵⁰ Fritz, M. C.; Hahner, G.; Spencer, N. D.; Burli, R.; Vasella, A. *Langmuir* **1996**, *12*, 6074-6082.

- ⁵¹ Biebuyck, H. A.; Bain, C. D.; Whitesides, G. M. *Langmuir* **1994**, *10*, 1825-1831.
- ⁵² Vance, A. L.; Willey, T. M.; Nelson, A. J.; Buuren, T.; Bostedt, C.; Terminello, L. J.; Fox, G. A. *Langmuir* **2002**, *18*, 8123-8128.
- ⁵³ Hostetler, M. J.; Stokes, J. J.; Murray, R. W. *Langmuir* **1996**, *12*, 3604-3612.
- ⁵⁴ Ulman, A. *Chem. Rev.* **1996**, *96*, 1533.
- ⁵⁵ Fendler, J. H. *Chem. Mater.* **1996**, *8*, 1616.
- ⁵⁶ Ulman, A. *Chem. Rev.* **1996**, *96*, 1533-1554.
- ⁵⁷ Sheppard, N.; Erkelens, J. *Appl Spectroscopy*, **1984**, *38*, 471-485.
- ⁵⁸ Shan-Yang, L.; Horng-Lun, C.; Yen-Shan, W. *J. Biomolecular Str & Dynamics* **2002**, *19*, 619-625.
- ⁵⁹ Liedberg, B.; Ivarsson, B.; Lundstroem, I.; Salaneck, W. R. *Progress in Colloid & Polymer Science* **1985**, *70*, 67-75.
- ⁶⁰ Hutt, D. A.; Leggett, G. J. *Langmuir* **1997**, *13*, 3055-3058.
- ⁶¹ O'Shea, J. N.; Schnadt, J.; Bruhwiler, P. A.; Hillesheimer, H.; Martensson, N.; Krempasky, J.; Patthey, L.; Wang, C.; Luo, Y.; Agren, H. *J. Phys. Chem. B* **2001**, *105*, 1917-1920.
- ⁶² Daniel, M-C.; Astruc, D. *Chem. Rev.* **2004**, *104*, 293-346.
- ⁶³ Weare, W. W.; Reed, S. M.; Warner, M. G.; Hutchison, J. M. *J. Am. Chem. Soc.* **2000**, *122*, 12890-12891.